AD-A162 758 MODELING ELECTROCARDIOGRAMS USING INTERACTING MARKOV CHAINS(U) MASSACHUSETTS INST OF TECH CAMBRIDGE LAB FOR INFORMATION AND D P C DOERSCHUK ET AL JUL 85 1/1

UNCLASSIFIED LIDS-P-1491 AFOSR-TR-85-1118 AFOSR-82-0258 F/G 6/5 NL

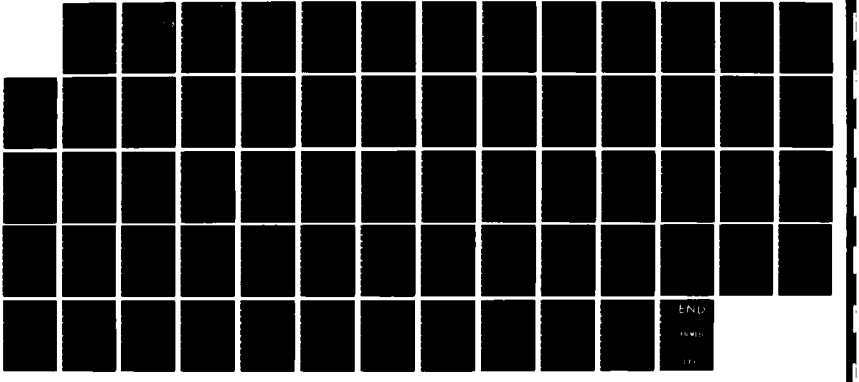

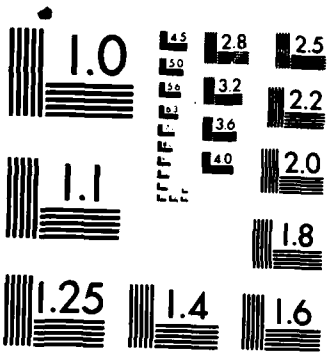

July 1985 LIDS-P- 1491

Modeling Electrocardiograms Using Interacting Markov Chains*

Peter C. Doerschuk**
Robert R. Tenney+
Alan S. Willsky±

Abstract

In this paper we develop a methodology for the statistical modeling of cardiac behavior and electrocardiograms (ECG's) that emphasizes (a) the physiological event/detailed waveform hierarchy; and (b) the importance of control and timing in describing the interactions among the several anatomical subunits of the heart. This metholology has been motivated by a desire to develop improved algorithms for statistical rhythm analysis that capture cardiac behavior in a more fundamental way but that stops short of complete accuracy in order to highlight decompositions that can be exploited to simplify statistical inference based on these models. Our models consist of interacting finite-state processes, where a very few of the transition probabilities for each process can take on a small number of different values depending upon the states of neighboring processes. Each finite-state process is constructed from a very small set of elementary structural elements. We illustrate our methodology by describing models for three cardiac rhythms and include simulation results for one of these, namely the rhythm known as Wenckebach.

*The research described in this paper was supported in part by the Air Force Office of Scientific Research under Grant AFOSR-82-0258. The first author was supported by fellowships from the Fannie and John Hertz Foundation and the M.D.-P.h.D. Program at Harvard University (funded in part by Public Health Service, National Research Award 2T 32 GM07753-06 from the National Institute of General Medical Science).

** Laboratory for Information and Decision Systems, M.I.T., Cambridge, MA, 02139 and Harvard Medical School, 25 Shattuck St., Boston, MA. 02115.

+ Laboratory for Information and Decision Systems, M.I.T., Cambridge, MA, 02139 and Alphatech, Inc., 2 Burlington Executive Center, 111 Middlesex Tpke., Burlington, MA, 01803

± Laboratory for Information and Decision Systems, M.I.T., Cambridge, MA, 02139.

6c. ADDRESS (City, State and ZIP Code) Cambridge, MA 02139	7b. ADDRESS (City, State and ZIP Code) Bldg. 410 Bolling AFB, D.C. 20332-6448

8a. NAME OF FUNDING/SPONSORING ORGANIZATION AFOSR	8b. OFFICE SYMBOL (If applicable) NM	9. PROCUREMENT INSTRUMENT IDENTIFICATION NUMBER AFOSR-82-0258

8c. ADDRESS (City, State and ZIP Code) Bldg. 410 Bolling AFB, D.C. 20332-6448	10. SOURCE OF FUNDING NOS.			
	PROGRAM ELEMENT NO.	PROJECT NO.	TASK NO.	WORK UNIT NO.
11. TITLE (Include Security Classification) Modeling Electrocardiograms Using Interacting Markov Chains	61102F	2304	A1	

12. PERSONAL AUTHOR(S)
P. C. Doerschuk, R. R. Tenney, A. S. Willsky

13a. TYPE OF REPORT Technical	13b. TIME COVERED FROM _____ TO _____	14. DATE OF REPORT (Yr., Mo., Day) July 1985	15. PAGE COUNT 63

16. SUPPLEMENTARY NOTATION

17. COSATI CODES			18. SUBJECT TERMS (Continue on reverse if necessary and identify by block number)
FIELD	GROUP	SUB. GR.	ECG's, Wenckebach rhythm, cardiac behavior, statistical inference

19. ABSTRACT (Continue on reverse if necessary and identify by block number)
In this paper we develop a methodology for the statistical modeling of cardiac behavior and electrocardiograms (ECG's) that emphasizes (a) the physiological event/detailed waveform hierarchy; and (b) the importance of control and timing in describing the interactions among the several anatomical subunits of the heart. This methodology has been motivated by a desire to develop improved algorithms for statistical rhythm analysis that capture cardiac behavior in a more fundamental way but that stops short of complete accuracy in order to highlight decompositions that can be exploited to simplify statistical inference based on these models. Our models consist of interacting finite state processes, where a very few of the transition probabilities for each process can take on a small number of different values depending upon the states of neighboring processes. Each finite state process is constructed from a very small set of elementary structural elements. We illustrate our methodology by describing models for three cardiac rhythms and include simulation results for one of these, namely the rhythm known as Wenckebach.

20. DISTRIBUTION/AVAILABILITY OF ABSTRACT UNCLASSIFIED/UNLIMITED ☐ SAME AS RPT. ☒ DTIC USERS ☐	21. ABSTRACT SECURITY CLASSIFICATION Unclassified

22a. NAME OF RESPONSIBLE INDIVIDUAL Dr. Marc Q. Jacobs	22b. TELEPHONE NUMBER (Include Area Code) (202) 767-4940	22c. OFFICE SYMBOL NM

I. Introduction

In this paper we describe a methodology for the statistical modeling of cardiac activity and electrocardiograms (ECG's). Our primary purpose in developing this methodology is to provide a basis for the design of automatic, statistical algorithms for rhythm analysis of ECG's, that is, the analysis of the sequential behavior of both atrial and ventricular events as observed in the ECG (see our companion paper (Doerschuk 1985b) where we describe our work on using these models to design ECG analysis algorithms).

Modeling of ECG's is certainly not a new endeavor (for reviews see Thomas 1979; Feldman 1977; Oliver 1977; LeBlanc 1973; Cox 1972; for further references see Proceedings of the IEEE Computers in Cardiology Conference, 1974-1984), nor is the development of statistical ECG models for the express purpose of designing signal analysis algorithms. However, the modeling methodology we describe here differs in a number of important ways from any earlier work. Roughly speaking what we have tried to do on the one hand is to overcome the limitations of existing signal processing models by capturing cardiac physiology in a far more fundamental way. On the other hand, we have stopped far short of the detail found in physiologically-accurate models and rather have aimed both to keep only enough detail to allow successful signal processing and to highlight several critical features found in physiological models that allow the development of computationally feasible algorithms.

In particular, as we briefly describe in the next section, the behavior of the heart is characterized by the occurrence of a small

number of events corresponding to contraction or relaxation of different major parts of the heart, and each of these events leads to the appearance of a particular waveform in the ECG. While very accurate descriptions of the ECG require breaking the ECG down further to account for the behavior of very small units of heart muscle, one can generally think of describing the ECG in an hierarchical fashion -- an upper level describing discrete, cardiac events and a lower level describing the impact these events have on the ECG. As we discuss at the start of Section 3, previously developed rhythm analysis methods typically make use of this decomposition implicitly -- i.e. only the event level description is modeled, and it is assumed that a wave detection preprocessor has been applied to the ECG to provide event-level inputs to the signal processing algorithms. Our approach differs from these in two important ways. In the first place, we explicitly model the two-level hierarchy, thereby allowing an integrated approach to wave detection and rhythm tracking. This provides one with a fundamental way in which to feed rhythm information back to the wave detection process (rather than in ad hoc fashions as can be found in some previous methods). Secondly, and more importantly, our event-level descriptions of cardiac behavior are far more detailed and accurate than those used previously (the importance of this for signal processing will be discussed later). In particular, the heart consists of several distinct subunits which interact relatively infrequently but strongly. Furthermore the coordinated action of the heart (or any particular anomaly) can be explained in terms of control and timing. Specifically, the contraction of one part of the heart initiates the contraction of a neighboring portion (and thereby controls its behavior)

if that portion of the heart is ready to contract (i.e. if the timing is right). As we describe, these observations plus a detailed examination of the mechanisms that characterize different cardiac rhythms have led us to develop a methodology for constructing spatially distributed models of cardiac behavior, emphasizing control and timing, and using a very small number of building blocks.

This paper is organized as follows. In the next section we provide a brief introduction to cardiac anatomy and physiology. In Section 3 we present an introduction to our modeling methodology and make some additional comments about its relationship to previous modeling approaches. Sections 4 and 5 describe the general mathematical structure of the upper and lower levels, respectively, or our models, and in Section 6 we describe in detail the several building blocks used to construct our upper level models. In Section 7 we present these examples of rhythm models using our methodology including the complete details and some simulations for one of these, namely the rhythm known as Wenckebach (Section 7.3).

2. Cariac Anatomy and Physiology

In this section we briefly describe the functioning of the heart, highlighting those aspects of cardiac physiology that are the keys to the coordination of cardiac activity and therefore to the description of cardiac rhythms. These features form the foundation of our approach to cardiac modeling. For far more complete descriptions of cardiac physiology see, for example, Chou (1979), Katz (1977), and Marriott (1977).

The pumping of blood by the heart is accomplished by the coordinated contraction and relaxation of cardiac muscle cells which in electrical terms correspond to the electrical depolarization and repolarization, respectively, of the cells. The initiation and coordination of this pumping activity

is accomplished by waves of electrical depolarization in the complex electrical conduction system embedded in the muscular and structural elements of the heart: the depolarization of one cell propagates to initiate the depolarization of neighboring cells along the heart's electrical pathways. An important fact is that after a depolarization, known as an action potential, passes through a particular patch of cell membrane, this portion of the heart goes through a process of repolarization during which it is at first completely and then relatively unresponsive to further attempts to initiate depolarization. This process lasts for on the order of 300 msec., and is known as the refractory period, and the two subdivisions are, respectively, the effective and relative refractory periods. The measurable effects of all of this electrical activity are the time-varying potential differences between fixed points on the surface of the body. These time-varying signals comprise the ECG.

Let us now describe the sequential behavior of the various parts of the heart that together produce a single, normal heartbeat. The first major feature of a heartbeat is the contraction of the atria, the upper chambers of the heart. The initiation of this contraction is accomplished by the sinoatrial node (the SA node). An important feature of many of the cells of the heart is that they are autorhythmic -- i.e. if they are not excited for some period of time by an external depolarization wave, they will undergo spontaneous depolarization and will continue to cycle through repolarization and depolarizatoin at a particular rate as long as no external wave interrupts the process. The cells in the SA node are autorhythmic, and in a normal heart, except for an occasional isolated

anomaly, they are the only autorhythmic cells that actually do undergo periodic spontaneous depolarization, thereby initiating and controlling the entire rhythmic beating of the heart. Following the depolarization of the SA node, the propagating action potential depolarizes the atrial muscle causing the contraction of the atria and generating a fluctuation in the ECG called a P wave (see Figure 1). Then the propagating action potential reaches the atrioventricular node (AV node) which, in a heart with normal anatomy, is the only electrical connection between the atria and the lower chambers of the heart, the ventricles. In the AV node, the depolarization wave travels with a much reduced velocity, leading to a delay of 70-80 msec. in traversing the node. This permits the filling of the ventricles prior to their contraction.

On leaving the AV node, the depolarization wave enters the specialized ventricular conduction system which, after several stages, terminates in the ventricular muscle. The depolarization of the ventricular muscle causes the contraction of the ventricles and generates a fluctuation in the ECG called an R wave (see Figure 1). Because the ventricular muscle mass is much greater than the atrial muscle mass, the R-wave potential fluctuations have much greater amplitude than those of the P wave and hence the R wave has a much higher signal to noise ratio than the P wave. As indicated in Figure 1, the Q and S waves are respectively the initial and final fluctuations associated with the R wave and the entire waveform is referred to as the QRS complex.

The repolarization of the atrial muscle, which occurs during the ventricular contraction, also generates a surface potential fluctuation.

This wave is smaller in amplitude than the P wave and is masked by the R wave generated by the ventricles. Finally, the ventricular muscle repolarizes which generates a fluctuation in the ECG called a T wave (see Figure 1).

From this description we can immediately see the several features described in the introduction. In particular, there is a natural hierarchical way in which to describe the ECG: an upper, event level and a lower level describing the actual waveforms resulting from those events. We also can see the spatially-distributed nature of the cardiac process, with the evolution of one portion of the heart affecting that of the next at those points in time corresponding to the propagation of a depolarization wave from one portion to the next. Intuitively, we might think of each portion of the heart as a clock that cycles through a sequence of states starting and ending at a resting state. For the autorhythmic SA node, transitions out of the resting state occur spontaneously, while in non-autorhythmic portions, such cycle-initiating transitions occur only when triggered by neighboring parts of the heart. Such a structure clearly displays the features of control and timing. Control here refers to one portion of the heart triggering activity in another. Timing refers to the fact that for this triggering to have an effect it is necessary for the second portion of the heart to be receptive to the excitation -- e.g. if it is in an effective refractory state, the depolarization wave will be terminated.

The preceding description is, admittedly, somewhat simplified. However, as we will demonstrate in this paper, not much additional complexity is needed to develop a methodology capable of modeling relatively complex cardiac rhythms. In particular, what is needed is to add a very few

additional features to the "clocks" describing the various parts of the heart. Specifically, there are three general mechanisms present in a physiologically normal heart, which, when combined with three broad categories of physiological abnormalities, lead to a wide variety of arrhythmias.

The first of these mechanisms has to do with autorhythmicity. As pointed out previously, many elements of the conduction system are autorhythmic. Those elements that are more distal[1] in the conduction system generally have lower rates. This relationship between location and rate is called the gradient of autorhythmicity. Thus there exists a competition between the SA node and other, distal, autorhythmic centers for control of the heart, that is, for which site will actually initiate cardiac depolarization. This leads us to the second important mechanism, reset/stunning. Specifically, when an autorhythmic cell is depolarized by the arrival of an external depolarization wave, the timer controlling when the next spontaneous depolarization will occur is reset. Therefore, in the normal heart, the faster SA node is able to retain control of the heart in spite of the competition from the other autorhythmic centers by continually resetting them before they have an opportunity to spontaneously depolarize. When a node is reset, the phenomenon called stunning can also occur where the time until the next spontaneous

[1] A distal structure is a structure that is depolarized late in the normal depolarization sequence. A proximal structure is depolarized earlier in the sequence.

depolarization is increased over the nominal time.

The third mechanism has to do with the direction of propagation of depolarization waves. While we have described unidirectional propagation of the depolarization wave through the conduction system in what is called the antegrade direction, the system is also capable of conduction in the reverse direction, called the retrograde direction. This is very important in cases when the cell membranes of the conduction system are not in a refractory state and a depolarization wave is initiated in a distal structure.

The three categories of physiological abnormalities are decreased conduction capabilities, increased or decreased rates of autorhythmicity, and abnormal electrical pathways connecting various portions of the heart (typically in the atrioventricular conduction pathway). Decreased conduction can occur in several different forms, for example, total block of all depolarization waves, unidirectional block of all depolarization waves coming from a particular direction, decreased propagation velocity, or increased refractory time. Increased (decreased) autorhythmicity refers to an increased (decreased) rate of autorhythmic depolarizations. Abnormal electrical pathwyas include several different structures that bypass all or part of the AV node and therefore have marked effects on cardiac timing. This small number of abnormalities, and mechanisms are commonly used to explain essentially all classes of cardiac rhythms. In Section 7 we illustrate this using the mathematical formalism we have developed for describing cardiac mechanisms, timing and control. Descriptions of many other rhythms in terms of these mechanisms can be found

in numerous texts. See also Doerschuk (1985a) for discussions of a number of additional rhythms and the description of models for several of these.

As a final point in this section we note that a very important aspect of abnormal cardiac physiology is that it is typically the interaction between the normal and abnormal parts of the heart that are of critical importance. That is, many of the changes in an arrhythmic ECG are due to how an abnormal substructure affects a normal part of the heart, rather than to a direct change in the ECG caused by the depolarization of the abnormal substructure. For example, the existence of a faster electrical connection between atria and ventricles leads to marked changes in the timing of the P and QRS waves and possibly to abnormal QRS complexes, even though the atria and ventricles are perfectly normal. This is another example of the importance of control in which the observed anomalies are caused by abnormal control of normal heart muscle. We will give other examples of this type in Section 7.

3. Introduction to the ECG Model

As we indicated in Section 1, modeling of ECG's is not a new topic. Numerous researchers have developed extremely detailed electromagnetic models of the heart either without particular attention paid to the time evolution of the sources of the electromagnetic activity (see, for example, (Geselowitz, 1979), (McFee, 1972), (Plansey, 1966, 1969, 1971, 1979), (Tripp, 1979) and (Wihswo, 1979)) or with time evolution as an important consideration (e.g. (Miller, 1978a, 1978b), (Vinke, 1977), (Moe, 1966), (Cohn, 1982) , (Smith, 1982), (Rosenberg, 1972), (Zloof, 1973), and (Thiry, 1974, 1975)). These modeling efforts had as their objective

developing detailed and physiologically accurate models of cardiac electrical activity and not developing models that could provide a useful basis for ECG signal processing. In particular these models generally are deterministic in nature or are only slightly removed from determinism (e.g. by allowing an initial, stochastic choice of parameters). Furthermore, the level of detailed included not only is far greater than is needed for signal processing purposes but also involves a far larger number of degrees of freedom than one could hope to identify using the very small number of measurement traces taken in a typical ECG. On the other hand, there are features in some of these efforts that we also include in our methodology. In particular, some of these models do employ hierarchical descriptions of cardiac timing and the actual electromagnetic effects, and they all generally treat the heart as an interconnection of (typically very large numbers of) submodels that interact infrequently but strongly.

Models that have been developed for signal processing purposes can be divided into two broad categories depending upon whether they model the sample-by-sample behavior of the ECG or just the sequential arrivals of the waves appearing in the ECG. Many authors (e.g. (Marcus, 1982), (Uijen, 1979), (Sornmo, 1981), and (Murthy, 1979)) have used sample-by-sample models of individual ECG beats, while others ((Borjesson, 1982), (Haywood, 1970), (Richardson, 1971)) have considered sample-by-sample models of complete rhythms. However, none of these models describe cardiac rhythms in the detail with which this paper is concerned.

Now let us briefly turn to event-based models. It is important to realize that the sequential index for such models is very different from that for sample-by-sample models. In a sample-by-sample model a data point $y(k)$ represents an ECG measurement at the kth time instant.

In an event-based model a data point represents the time interval between the kth occurrence of one type of wave and the next occurrence of that or another specified type of wave. In most of these models only the intervals between successive R waves (corresponding to ventricular contractions) are considered. In one set of models, these R-R intervals are quantized into several classes. In most cases only 3 classes -- short, regular, or long -- are considered, and various rhythms are described either by use of Markov chains ((Gersch, 1970, 1975), (Tsui, 1975), (Shah 1977), (White, 1976)) or deterministic finite automata (Hristov, 1971) to model the evolution of R-R interval patterns. In another set of papers (Gustafson, 1977, 1978a, 1978b, 1978c, 1979, 1981) interval lengths are not quantized, and an extensive set of vector Markov models are developed to describe the evolution of event interval patterns (see (Ciocloda, 1983) for an independent, though less comprehensive development). In the first part of this work (Gustafson 1977, 1978a, 1978b) only R-R intervals are considered, while P-R intervals are also considered in the later papers.

From the perspective of the approach taken in this paper, these event-oriented models do highlight the timing information, which is of primary importance in tracking or identifying cardiac rhythms. However, the use of purely event-based models has some fundamental limitations. In Section 1 we mentioned one of these, namely the implicit assumption that wave detection has already been performed in a preprocessor. As we indicated, one might expect superior performance in an integrated algorithm in which rhythm tracking information assists wave detection. Only in (Gustafson, 1979) does one find an ad hoc use of feedback from tracker to

wave detector. While the absence of a fundamental way in which to effect this feedback is a limitation, it is not the most serious one. A more basic problem with event-based models is the limited way in which one must model preprocessor errors. Specifically, this framework allows one to model the error in measuring the interval between two events, but it cannot accommodate the possibility that one of these events is missed altogether by the preprocessor. While this is not a serious problem for the large-amplitude QRS complex, it is a serious problem for a much smaller P-wave. The difficulty here is with the sequential event-related index, and the use of this index creates another even more serious problem. In particular in many cardiac rhythms, such as those involving some type of A-V node abnormality that on occassion causes a ventricular contraction to be dropped, there are a variable number of P waves between successive R-waves. For rhythms such as these the use of an event-oriented time index breaks down or at best leads to models with a tenuous connection to actual cardiac behavior.

In our approach to cardiac modeling we have also attempted to highlight the occurrence of cardiac events as has been done in these previous signal processing models. However, we have at the same time avoided the difficulties described previously by basing our models far more closely on cardiac physiology and anatomy. Our models rely heavily on spatial, temporal, and hierarchical decompositions. The spatial and temporal decompositions are well-founded physiologically in that they are based on the anatomic division of the heart into subunits within which events occur at a far greater rate than do interactions between subunits. While

the framework we have developed for exploiting these two decompositions is rich enough to allow one to consider extremely fine anatomic subdivisions (such as those considered in the physiologically-accurate models described previously) using the small number of building blocks we will describe, we have generally found it necessary to consider decompositions into only a few submodels (e.g. one for the SA node, one for the atria, one for the AV node, etc.).

The hierarchical decomposition we have developed is not entirely accurate physiologically but is similar in spirit to other modelling approaches and is flexible enough to allow us to mimic cardiac behavior quite accurately. Its two levels are based on a separation of discrete cardiac events and timing from the generation of the actual ECG waveforms. This hierarchy separates the high-level events we wish to detect and track from the actual observed voltages, and this separation is useful for signal-processing purposes.

Figure 2 presents a three-submodel example of the type of model we consider. The square boxes at the upper level of the hierarchy comprise the discrete-state physiological model, which captures the sequential evolution of high level events in the heart. The mathematical structure of these models is described in Sections 4 and 6. Each submodel represents a functional anatomic structure (e.g. the atria, the ventricles, etc.). The directed solid lines indicate the initiator and recipient of control inputs, which we call interactions. For example, the transmission of a depolarization wave from atria to AV node might be modeled

via an interaction in which the present state of a submodel representing the atria causes a transition in the AV-nodal submodel, representing the initiation of the AV-nodal depolarization.

The triangular objects in Figure 2 are parts of the electromagnetic model which models the actual observed waveforms. Each submodel corresponds to the generation of the ECG contribution from a particular antomic structure of the heart (e.g. P waves from the atria). The dashed lines indicate the control of the electromagnetic level by the physiological level of a single submodel. These inputs are used to initiate the generation of waveforms in the observed ECG. For example, the occurrence of a particular transition in the physiological portion of an atrial submodel might initiate the generation of a P wave in the corresponding electromagnetic submodel. The mathematical structure of the electromagnetic level is described in Section 5. Note that the electromagnetic level does not affect the physiological level and that no electromagnetic submodel affects any other electromagnetic submodel. Note also that the unidirectional interactions between levels occur only between the two levels of a single submodel (i.e. events in a submodel corresponding to the atria cannot initiate an R wave).

Finally, recall from Section 2 that the abnormal aspects of an arrhythmic ECG occur because there is some abnormal anatomic substructure in the heart which makes a direct abnormal contribution to the ECG and/or interacts with other normal parts of the heart causing them to make an abnormal contribution to the ECG. In our models of arrhythmias, we take the same approach. That is, we begin with a normal rhythm model which is transformed into an arrhythmia model by altering the appropriate submodel. The contribution of the altered submodel and its interactions with the unaltered submodels create th

arrhythmic ECG. In order for the interactions to occur, we often must generalize the normal submodels. The alterations are to include properties which were left out initially because, in the normal rhythm, they represented unnecessary detail.

4. The Upper Hierarchical Level

In this section we discuss the upper hierarchical level, which we call the physiological model. This level is concerned with discrete events, and we have chosen to use Markov chains to describe their evolution. Because of the importance of spatial decompositions, we have also chosen a highly structured class of chains described in the following.

The state space of our Markov chains is the cross product of a set of spaces corresponding to the "states" of subprocesses which comprise the overall chain. Each subprocess corresponds to one of the anatomic subunits of the heart. Furthermore, there is a direct correspondence between each state of a subprocess and a physical state of the corresponding anatomic subunit. We call each subprocess a submodel. We often refer to an element in the subprocess "state" space as a state, and, in an abuse of terminology we often refer to the individual subprocesses as Markov chains.

Let x_n be the state of the overall Markov chain which consists of a set of N subprocess denoted x_n^i, i=0,...,N-1 and let p(n) be the pmf on x_n. Since x_n is a Markov chain, p(n+1)=Ap(n) where A is a stochastic matrix. That is, the elements of A are the values of $p(x_{n+1}|x_n)$ as x_n and x_{n+1} range over all allowed values.

A key feature of our models is that $p(x_{n+1}|x_n)$ has a great deal of

structure. Specifically:

(1) Given x_n, the transitions of each of the component subprocesses are independent. That is,

$$p(x_{n+1}|x_n) = p(x^i_{n+1},\ i=0,\ldots,N-1|x_n) = \prod_{i=0}^{N-1} p(x^i_{n+1}|x_n).$$

(2) For each subprocess there are far fewer values of $p(x^i_{n+1}|x_n) = p(x^i_{n+1}|x^j_n,\ j=0,\ldots,N-1)$ than there are values of $\{x^j_n,\ j\neq i\}$. That is, we assume that $p(x^i_{n+1}|x_n) = p(x^i_{n+1}|x^i_n,h^i_n)$ where $h^i_n = h^i(x^h_n,\ j\neq i)$ denotes the net interaction of all other subprocesses with the i^{th} subprocess. Here h^i_n may take on values 0, 1, 2, ... but the assumption is that the number of possible values of h^i_n is far less than the number of possible values of $\{x^j_n,\ j\neq i\}$. In fact in our examples h^i_n takes on at most 2 or 3 values and only one or two transition probabilities of the ith chain are affected by the value of h^i_n. Thus, the subprocesses are "almost" independent, but, as we will see, these interactions can have an extremely important effect on the evolution of the subprocesses.

We now consider a very simple model for normal rhythm in order to fix these ideas about interacting subprocesses. This model has two submodels, corresponding to a division of the heart into two anatomic substructures: the SA-atrial (SA/A) substructure, composed of the SA node and atria, and the AV-ventricular (AV/V) substructure, composed of the AV junction and ventricles. As in the normal heart, the SA/A submodel originates interactions with the AV/V submodel, corresponding to a super-ventricular depolarization originating in the SA node and propagating through the AV junction in an antegrade direction. For simplicity,

the reverse (retrograde) conduction is not modeled.

In the SA/A submodel (Figure 3(b)), the state transition from 0 to 1 represents the firing of the SA node and the atrial depolarization. The time required for the state to travel from state 1 to state 0 models the random time between successive depolaraizations of the autorhythmic SA node. Finally, by assuming that the atrial conduction velocity is infinite (an oversimplification for the purpose of illustration only), state 1 also represents the excitation of the AV node by the atrial depolarization.

That state 1 (in the SA/A submodel) represents the excitation of the AV node is reflected in the differing probabilities assigned in the AV/V submodel (Figure 3(c)) depending on whether the SA/A-submodel state is or is not in state 1. AV/V-submodel state 0 represents the fully repolarized state of the AV node and ventricles. If the AV/V submodel is in that state and the SA/A submodel moves into state 1, then the AV/V-submodel state transitions into state 1 with probability 1. This transition models the excitation of the AV node by the atrial depolarization. If the AV/V substructure is not receptive to a depolarization (i.e. is refractory), then the submodel state will not be in state 0 and the change in the probabilities due to the SA/A-submodel state occupying state 1 will have no effect on the evolution of the AV/V subprocess. The time required in the AV/V submodel for the state to travel through states 1 and 2 represents the (deterministic) AV-junctional delay time. The transition from state 2 to state 3 represents the initiation of ventricular depolarization. Finally, the time required for the state to

travel through states 3, 4, and 5 represents the (random) AV-junctional and ventricular repolarization time. After the repolarization is complete, the state traps in state 0 awaiting another excitation from the SA/A submodel.

5. The Lower Hierarchical Level

We now discuss the lower level in our hierarchy, which we call the electromagnetic model. The spatial decomposition that was imposed on the upper hierarchical level is also imposed on the lower hierarchical level. As in the upper hierarchical level, we use the term submodel for the decomposed elements. The reason that the hierarchical decomposition carries through is that the individual waveforms in the ECG that are modeled by the electromagnetic level are each due to a single anatomic subunit.

Each state of each physiological submodel has a physical interpretation. Certain transitions between states correspond to the initiation of waves, so these transitions are used to drive the corresponding electromagnetic submodel. The output of each of the electromagnetic submodels is a linear superposition of signals with shifted origins. The unshifted signals are called signatures. The origin is the time at which the initiating transition in the corresponding physiological submodel occurs. Each signature is a shift-invariant finite-durational deterministic function with additive white zero-mean Gaussian noise (signature noise), where the additive noise is independent from one occurrence of the signature to the next and represents beat-to-beat variations. Finally, the outputs of the individual eletromagnetic

submodels are linearly superposed and the result is observed in additional, exogenous, white Gaussian noise (observation noise).

Let $S^i_{j,k}$ be the signature from the i^{th} electromagnetic submodel when the i^{th} physiological submodel makes a transition from j to k. Let v be the white Gaussian observation noise. The observation y is then†

$$y(t) = \sum_i \sum_n S^i_{x_{n-1},x_n}(t-n) + v(t).$$

Consider again the example of the previous section. In the S/A submodel (Figure 3(b)), as discussed previously, the state transition from 0 to 1 represents the firing of the SA node and the atrial depolarization. Thus, as indicated in the diagram, the electromagnetic-model response to this transition is the P wave of the ECG. The electromagnetic-model response to the other state transitions, e.g. from 2 to 3, is identically zero and hence is not indicated.

In the AV/V submodel (Figure 3(c)), as discussed previously, the state transition from 2 to 3 represents the initiation of the ventricular depolarization. Hence the electromagnetic-model response to the corresponding transition is the QRS complex and the T wave. Here, we are modeling the QRS complex and T wave as deterministicly coupled waveforms -- the ST interval duration is not random. Note that a more complex model of the same type could allow a random coupling. The

---

† This equation represents an abuse of notation. Specifically, each occurrence of a particular signature includes signature noise independent of the noise in other occurrences. Thus the various occurrences of S^i_{jk} are not identical (although the deterministic mean is the same).

electromagnetic-model response to the other state transitions is identically zero and hence is not indicated.

Several aspects of the electromagnetic model merit comment.

(1) Note that some anatomic subunits do not cause waves in the ECG (e.g. the AV nodes) and therefore the corresponding electromagnetic submodel does not exist. Similarly, most transitions in our physiological submodels model the timing between wave and interaction initiations and therefore have no effect on the corresponding electromagnetic submodel. Thus very few transitions actually contribute to the ECG.

(2) The randomness in the signatures models the beat-to-beat variation in the morphology of the ECG waveforms for a single subject. Clearly one could consider a more complex correlated model for the signature noise in order to model these variations more realistically. In addition, by augmenting particular subprocess state spaces and allowing the additional transitions to initiate different versions of the same signature, different morphologies for the same wave can be included.

(3) The additive white Gaussian noise v that is added to the summed output of the electromagnetic submodels models all noncardiac contributions to the observed signal (e.g. contributions due to other muscles, measurement errors and noise, etc.).

(4) The Markov chain cycle interval need not equal the signature sampling interval. Typically, the Markov chain cycle interval can be taken to be substantially larger than the signature sampling

interval reflecting the difference in time scale between interaction events (which determine the Markov chain cycle interval) and events internal to the anatomic submodels (which set the signature sampling interval). Because signatures can only be initiated at Markov chain cycles, unequal intervals appear to imply that signatures cannot be initiated at arbitrary signature samples. However, by using an augmentation technique as in (2), this problem can be overcome. For an example, see the Wenckebach model of Section 8.

6. The Microscopic Model -- Structural Elements

In this section we describe the small number of elementary structural elements that are used in constructing the various submodels of our physiological models. Each of these elements is a piece of a Markov chain. There are two fundamental structural elements, which are essentially elapsed time clocks, out of which three other structural elements are constructed.

The first structural element is the delay line (DL). When the state of a chain enters the first state of such an element, denoted i, it undergoes a random time delay and then arrives at the final state denoted o. The delay is called the transit time. The pmf on the transit time is specified and unaffected by events in the other chains. In block diagrams we use the symbol shown in Figure 4 for a DL. The DL should be viewed as a piece of an overall chain. Here the arrows at either end of the DL indicate transitions into the initial state i from other states in the overall submodel (possibly including 0) and from the final state 0 to other states (possibly including i). No transitions exist to or from external states to states internal to the DL. The DL is used to model simple timing behavior in the coordinated operation of the

heart. Two examples of DL's are displayed in Figure 5. In the first of these there are no feedback transitions so that the transient time is bounded by the length of the DL. In the second example the presence of feedback transitions implies that there is in principle no upper bound on the transit time. In both examples the transit time pmf can be adjusted by varying the several transition probabilities.

The second structural element is the resettable delay line (RDL). This element is used to model both timing and the reset and stunning phenomena that can occur when a depolarization wave reaches an autorhythmic site. We often use the term delay line as a generic name for both DLs and RDLs. The differences between the RDL and the DL are that there are two different mechanisms for the state to exit an RDL, and an RDL has transition probabilities that are controlled, in a very simple and specific way, by interactions initiated by another subprocess in the overall Markov chain. Specifically, the possible interactions impinging on a chain containing an RDL are divided into two classes denoted normal and abnormal. Within each class the transition probabilities in the RDL are constant. When the interaction is in the normal class, the RDL behaves as DL, transiting from the initial state i toward the final state 0 as long as the interaction remains in the normal class. However, when the interaction is in the abnormal class, a second set of transition probabilities is used for the next transition. The second set of transition probabilities forces the state to leave the RDL and enter a state, external to the RDL, called the reset state and denoted by r.

In block diagrams we use the symbol shown in Figure 6 for an RDL. Here the dashed arrow and symbol c denote the effect of interactions from other submodels. The variable c takes on two values: R (for "reset") if the current impinging interaction is in the abnormal class and $\overline{R}$ (for "not reset") otherwise. An example of an RDL is given in Figure 7.

The third structural element is the autorhythmic element which is capable of sustained cyclic behavior without external excitation. This element is constructed from DL(s) and/or RDL(s). The basic idea is to attach the input and output of a DL together, as in Figure 8. If an DL is used, then this specifies the entire chain. If an RDL is used, then it is also necessary to specify the identity of the reset state (see the example in Section 8.2). The choice of DL versus RDL depends on what physiological process is being modeled. Typically one or more transitions in the autorhythmic element will initiate signatures in the ECG (corresponding, for example to the P wave resulting from the autorhythmic operation of the SA node).

The fourth structural element is the passive transmission line (PTL). This element is constructed from a DL or an RDL. We illustrate the DL case in Figure 9. A PTL is a connection of a single state, called the resting state, to the initial state of a DL. The only allowed transition out of the resting state is into the DL. The transition probability for this transition, denoted p, depends on the value of the current interaction impinging on the submodel containing the PTL. The possible values of the implinging interaction are partitioned into two disjoint sets called the autonomous and nonautonmous sets. When the

current impinging interaction is in the autonomous set, p=0. That is, the resting state is a trapping state. In the other case (nonautonomous), p>0. The PTL can be used to model a part of the heart, such as the AV node, that begins depolarization (i.e. enters the delay line) only when an external depolarization wave excites it. Again it is possible that one or more transitions in the PTL will generate signatures in the ECG.

The fifth structural element is the bidirectional refractory transmission line (BDRTL), shown in Figure 10, which is a complete submodel in itself and is used to model structures capable of supporting conduction in either the antegrade or retrograde direction. All unlabeled transition probabilities in Figure 10 take on the value 1. The state 0 corresponds to the repolarized resting state of the anatomic substructure. The RDL labeled A (R) corresponds to antegrade (retrograde) conduction. In accordance with these designations, the BDRTL attempts to excite the submodel(s) corresponding to the adjacent distal (proximal) anatomic substructure(s) whenever the BDRTL state occupies state o_A (o_R), the final state of the antegrade (retrograde) conduction RDL. RDLs are used here in order to model the possible collision of two depolarization waves, one in the antegrade and one in the retrograde direction. The relationship between the resting state 0 and the RDLs A and R is a simple generalization of the PTL structural element. The third delay line (F), a DL, corresponds to the refractory period. A nonresettable delay line is used because, at the level of physiological detail that we are modeling, the duration of the refractory period is independent of all external events.

The state transition probabilities $p_{0,A}$, $p_{0,R}$, and $p_{0,F}$ and the RDL

state transition probabilities (controlled exclusively through c_A and c_R) are the only probabilities that depend on the states of other submodels, that is, on the interactions impinging on the BDRTL. In the absence of external excitations, $p_{0,A} = p_{0,R} = p_{0,F} = 0$ and $c_A = c_R = \overline{R}$. That is, under these conditions, if the process was in the resting state, it remains there until an extended excitation initiates depolarization. If the process was in the middle of a depolarization, the depolarization continues in a normal fashion. If the BDRTL is excited from the antegrade direction but not simultaneously from the retrograde direction, then $p_{0,A} = 1$, $p_{0,R} = p_{0,F} = 0$, $c_A = \overline{R}$, and $c_R = R$. In this case if the process was in the resting state, it immediately exits and begins an antegrade depolarization. If the process is in the middle of a retrograde depolarization, the depolarization is stopped by restting the RDL. This models the collision of the two depolarization waves. After this point in time the process proceeds through the DL modeling the refractory period. For the reverse case (i.e. excited from the retrograde direction but not simultaneously from the antegrade direction), the values are $p_{0,R} = 1$, $p_{0,A} = p_{0,F} = 0$, $c_R = \overline{R}$, and $c_A = R$. Finally, if the BDRTL is simultaneously excited from both the antegrade and retrograde directions, the $p_{0,F} = 1$, $p_{0,A} = p_{0,R} = 0$, and $c_A = c_R = R$.

Depending on what anatomic substructure the BDRTL models, it may or may not contain transitions which generate a non-zero response in the electromagnetic model (e.g. if the BDRTL models the AV node, no signature will be generated by this submodel). If the BDRTL does contain such transitions, then there are three basic situations which we illustrate assuming that the BDRTL models the atria which can be excited by the SA node or by retrograde conduction from the AV node. The three situations

in which signatures are generated correspond to

(1) Antegrade condution without a reset (e.g. a normally conducted P wave from the SA node through the atria).

(2) Retrograde conduction without a reset (e.g. a retrograde P wave from the AV node through the atria).

(3) Reset-antegrade or retrograde conduction, corresponding to collisions of two depolarization waves. Such an occurrence generates a so-called fusion depolarization (e.g. a fusion P wave due to joint SA-nodal and retrograde-AV-junction deplorizations).

Though it is not the only possiblity, we have always used the transition from the resting state to i_A or i_R to generate the nonreset antegrade and retrograde electromagnetic model responses. For simplicity in our work, we have assumed that a fusion depolarization is identical to the response from the earlier of the two depolarization waves. Models allowing for a different signature for fusion waves, can be easily generated with only slight modifications.

7. Examples of ECG Models

The small number of building blocks described in the preceding section can be used to construct models for any cardiac rhythm. In our work (Doerschuk, 1985a), for example, we have shown how one can relatively easily write down models for cardiac arrhythmias involving re-entrant pathways (in which depolarization waves can in fact cycle through parts of the heart several times), abnormal atrial-ventricular conduction pathways (such as the so-called Wolff-Parkinson-White syndrome), and the presence of ectopic foci (autorhythmic sites other than the SA node with increased autorhythmic rates that allow them to compete successfully

with the SA node. In this section we illustrate our methodology by presenting models for three different cardiac conditions: normal rhythm, normal rhythm with ectopic focus PVCs, and second degree AV block (Mobitz Type I), also called Wenckebach. The first two models are specified at the level of the structural elements described in the previous section, while the third is described in complete detail.

A simple, graphical, abstract notation for classes of models is helpful in describing the models. This paragraph describes such a notation by example. Figure 11 illustrates a model made up of four submodels. The boxes labeled C0, ..., C3 denote these submodels. The directed lines between boxes indicate the existence of an interaction in the indicated direction. Thus, for example, submodel C0 initiates an interaction with submodel C1. The number of values which the interaction can take on is not specified. The wavy lines terminating in S0, ..., S3 indicate that the submodel of the originating box contains one or more transitions which initiate a signature whose name is the label at the end of the arrow.

8.1. Normal Rhythm

The rhythm modeled in this subsection is a prototypical normally conducted rhythm. A block diagram of the model and a listing of the intersubmodel interactions is given in Figure 12. As seen in Figure 12, the heart is divided into four anatomic substructures--SA node, atria, AV junction, and ventricles--each of which is modeled by a separate submodel.

Qualitatively, the model behaves in the following manner. The SA-nodal submodel initiates a depolarization wave. This is the only way in

which a depolarization can be initiated in this model. The depolarization then propagates antegrade through the atrial submodel, producing the P wave; the AV-junctional submodel, which makes a zero contribution to the ECG; and finally the ventricular submodel, producing a QRS-T complex.

Because only antegrade conduction is included in the model, submodel 0 is not resettable and submodels 1 and 2, which would be BDRTLs if retrograde conduction were included, are instead simple arrangements of delay lines.

8.2. Normal Rhythm with Ectopic Focus PVCs

As we have mentioned previously, there are numerous autorhythmic sites in the heart, and occasionally, even in a normal heart, one of these sites may successfully initiate a depolarization wave. Such a site is referred to as an ectopic focus or pacemaker. If this focus is located in the ventricles, what can result is the contraction of the ventricles a short time before the next normal depolarization would have occurred. Such a beat is called a premature ventricular contraction (PVC).† Because of the anomalous location at which this depolarization starts (typically in one ventricle or the other), the resulting QRS waveform is generally quite different from a normal beat. Typically the PVC is a more spread-out waveform as the initiation of the contraction of one

† PVC's can also arise through a reentrant pathway mechanism. In this case there is typically a more regular relationship between the timing of the PVC and the previous, normal QRS complex. It is certainly possible to model this mechanism using our methodology, but we do not do so here.

ventricle precedes that of the other by a noticeably larger time interval. Furthermore, when a PVC occurs, it is possible for the resulting depolarization wave to propagate in a retrograde direction. This depolarization wave may collide with the normal SA-node-initiated wave or it may complete a retrograde depolarization through the AV node and atria, finally arriving at and resetting the SA node.

In order to develop a model for this arrhythmia, we have modified the normal-rhythm model in two ways. First, we have modified the part of the normal-rhythm model which corresponds to the part of the heart which exhibits the abnormal physiology. Therefore we have replaced the ventricular submodel by a new ventricular submodel and an ectopic ventricular pacemaker submodel. Second, we have modified, as required, the remaining parts of the normal-rhythm model so that they can interact with the part modified in the first step. The primary purpose of these modifications is to allow retrograde conduction and resetting of the SA node. A block diagram of the model and a listing of the inter-submodel interactions is given in Figure 13.

8.3. Wenckebach

Wenckebach is characterized by a multibeat cycle in which the P waves are repeated at constant intervals but the P-R interval grows until, in the final beat of the cycle, the R wave is dropped. Then the cycle begins again with the P-R interval reset to its initial small value. The increase in the P-R interval from beat to beat is usually greatest at the beginning of the multibeat cycle. The multibeat cycle is typically three or four beats long.

Physiologically, the cause of Wenckebach is a defective AV node. Specifically, the AV node is such that it has a long relative refractory period. At the beginning of the multibeat Wenckebach cycle, the AV node is at rest. The first excitation occurs and is transmitted to the ventricles and the AV node enters its refractory period. Because the refractory period is prolonged, the second excitation from the atria reaches the AV node during its relative refractory period. The impulse is still able to excite the AV node (although propagation is at a reduced speed) and through it the ventricles, since the effective refractory period is past. However, the early excitation of the AV node has two effects: the following P-R interval and the following refractory period are both prolonged. Thus the third excitation occurs even earlier in the relative refractory period. This lengthening of the P-R interval and refractory period continues until finally a depolarization wave attempts to excite the AV node during its effective refractory period and is not conducted at all. This leads to the dropped R wave. Because the AV node is not excited during the dropped beat, the occurrence of the dropped beat gives the AV node time to complete its refractory period. Therefore, the P-R interval and refractory period for the succeeding depolarization of the AV node are reset to their initial (i.e. small) values.

We now describe the behavior of the AV-nodal (AV) submodel during a Wenckebach cycle (see Figure 14 and, for more detail, Figure 15). Initially the AV node is at rest: $x^1=0$. When the AV submodel is

excited, the state transitions into the AV_1 DL. The transit time for this DL is the AV-junctional delay. A transit time from the AV_1 DL is biased toward shorter values than a transit time from any of the other AV_i DLs. Therefore, as desired, this is the shortest possible AV-junctional delay. After the AV-junctional delay, the AV submodel attempts to excite the V submodel: $x^1=1$. Then the AV submodel enters the effective refractory period. Note that the effective refractory period contains a transit-time contribution only from the AR_4 DL and therefore the effective refractory period is short. Following the effective refractory period is the relative refractory period consisting of the total time spent in the RR_1, RR_2, and RR_3 DLs. If the next excitation of the AV submodel is sufficiently delayed, the AV submodel's state will pass through the three RDLs labeled RR_1, RR_2, and RR_3 and reenter the resting state (state 0). However, that is not what usually occurs. Rather, the refractory period duration is such that the next excitation of the AV submodel generally occurs during the relative refractory period. More specifically, because this first beat of the cycle had a short AV-junctional delay (using delay line AV_1) and a short effective refractory period (avoiding delay lines AR_1, AR_2, and AR_3), the next excitation of the AV submodel genreally occurs while the AV submodel's state is in the final RDL of the relative refractory period, namely RR_3. Therefore, the excitation of the AV submodel forces the AV submodel's state to transition into the AV_2 DL, leading to a somewhat longer AV-junctional delay than in the first beat of the cycle and subsequently to a somewhat longer effective refractory period (AR_3 and AR_4 delay lines).

In this state of the cycle the state is typically in the RR_2 DL when the following excitation occurs. Therefore, the state is reset into the AV_3 DL. This leads to a still longer AV-junctional delay (AV_3 delay line) followed by a longer effective refractory period (AR_2, AR_3, and AR_4 delay lines). The state is typically in the RR_1 RDL when the following excitation occurs. Therefore, the state is reset into the AV_4 DL producing a long AV-junctional delay followed by a long effective refractory period (AR_1, AR_2, AR_3, and AR_4 delay lines). In this part of the cycle the state is typically still in one of the effective-refractory-period DLs when the following excitation occurs. Therefore this excitation has no effect on the AV submodel. Rather, the state of the AV submodel continues through the effective-refractory-period DLs, the relative-refractory-period RDLs, and finally traps in the resting state (state 0). It remains in the resting state until the succeeding excitation occurs. Therefore, the excitation which should have started beat five does not get passed on to the ventricles. That is, beat five is dropped. Finally, because the state of the AV submodel is able to reach the resting state (state 0), the Wenckebach cycle is restarted.

The actual Markov chains and signatures are shown in Figure 16. They were chosen based on a nominal heart rate of 60 beats per minute with a Markov chain cycle period of 1/25 second and a signature sampling period of 1/100 second. Note the multiple copies of the P wave signature with one, two, or three leading zeros. These were introduced so that P waves could begin at any signature sample rather than at only every fourth signature sample (i.e. at a Markov chain transition).

Similar remarks apply to the V and T waves in the V submodel.

Table 1 gives a summary of a few successive Wenckebach periods. Note the lengtheing P-R intervals followed by a dropped beat. Note also that the model is not deterministic. For example, sometimes the Wenckebach cycle is four beats long and sometimes it is five.

Finally, Figure 17 gives the actual simulated ECG corresponding to the data in Table 1.

Acknowledgements

We are grateful to Prof. R.G. Mark for the opportunity to use the M.I.T. Biomedical Engineering Center's computational facilities.

References

(Borjesson, 1982)
P. O. Borjesson, O, Pahlm, L. Sornmo, and M.-E. Nygards, "Adaptive QRS Detection Based on Maximum A Posteriori Estimation", IEEE Trans. on Biomed. Eng., Vol. BME-29, No. 5, pp. 341-351, May, 1982.

(Chou, 1979)
T.-C. Chou, Electrocardiology in Clincal Practice (New York: Grune and Stratton, 1979).

(Ciocloda, 1983)
Gh. Ciocloda, "Digital Analysis of RR Intervals for Identification of Cardia Arrhytmias", Section 11. Int. J. Bio-Medical Computing, Vol. 14, pp. 155-169, 1983.

(Cohn, 1982)
R. L. Cohn,S. Rush, and E. Lepeschkin, "Theretical Analyses and Computer Simulation of ECG Ventricular Gradient and Recovery Waveforms", IEEE Trans. on Biomed. Eng., Vol. BME-29, No. 6, pp. 413-423, June, 1982.

(Cox, 1972)
J. R. Cox Jr., F. M. Nolle, and R. M. Arthur, "Digital Analysis of the Electroencephalogram, the Blood Pressure Wave, and the Electrocardiogram", Proc. IEEE, Vol. 60, No. 10, pp. 1137-1164, Oct., 1972.

(Doerschuk, 1985a)
P. C. Doerschuk, "A Markov Chain Approach to Electrocardiogram Modeling and Analysis", Ph.D Thesis, Dept. of Electrical Engineering and Computer Science, M.I.T., Cambridge, MA., June, 1985.

(Doerschuk, 1985b)
P. C. Doerschuk, R. R. Tenney, and A. S. Willsky, "Model-Based Rhythm Classification of Electrocardiograms Using Interacting Markov Chains", in preparation.

(Feldman, 1977)
C. L. Feldman and M. Hubelbank, "Cardiovascular Monitoring in the Coronary Care Unit", Med, Instrum. (USA), Vol. 11, No. 5, pp. 288-292, Sept.-Oct., 1977.

(Gersch, 1970)
W. Gersch, D. M. Eddy, and E. Dong Jr., "Cardiac Arrhythmia Classification: A Heart-Beat Invertal-Markov Chain Approach", Comput. and Biomed. Res. (USA), Vol. 4, pp. 385-392, 1970.

(Gersch, 1975)
W. Gersch, P. Lilly, and E. Dong Jr., "PVC Detection by the Heart-Beat Interval Data-Markov Chain Approach", Comput. and Biomed. Res. (USA), Vol. 8, pp. 370-378, 1975.

(Geselowitz, 1979)
D. B. Geselowitz, Magnetocardiography--An Overview", IEEE Trans. on Biomed. Eng., Vol. BME-26, No. 9, pp. 497-504, Sept., 1979.

(Gustafson, 1977)
D. E. Gustafson, A. S. Willsky, J.-Y. Wang, M. C. Lancaster, and J. H. Triebwasser, "A Statistical Approach to Rhythm Diagnosis of Cardiograms", Proc. IEEE, Vol. 65, No. 5, pp. 802-804, May, 1977.

(Gustafson, 1978a)
D. E. Gustafson, A. S. Willsky, J.-Y. Wang, M. C. Lancaster, and J. H. Triebwasser, "ECG/VCG Rhythm Diagnosis Using Statistical Signal Analysis, Part I: Identification of Persistent Rhythms", IEEE Trans. on Biomed. Eng., Vol. BME-25, No. 4, pp. 344-353, July, 1978.

(Gustafson, 1978b)
D. E. Gustasfson, A. S. Willsky, J.-Y. Wang, M. C. Lancaster, and J. H. Triebwasser, "ECG/VCG Rhythm Diagnosis Using Statistical Signal Analysis, Part II: Identification of Transient Rhythms", IEEE Trans. on Biomed. Eng., Vol. BME-25, No. 4, pp. 353-361, July, 1978.

(Gustafson, 1978c)
D. Gustafson, J. Wang, W. Kessel, A. Akant, A. Willsky, S. Mitter, P. Doerschuk, and S. Zisk, "Investigation of Signal Analysis Techniques for ECG/VCG Classification, Vol. I: Analytical and Numerical Studies", Final Report to USAFSAM, Brooks AFB, Texas 78235 for contract F33615-77-C-0606, Scientific Systems, Inc., Cambridge, MA, Report S2I TR 78-2, Jan., 1978.

(Gustafson, 1979)
D. Gustafson, J. Wang, S. Gelfand, J. Rood, A. Willsky, and S. Mitter, "Computerized ECG Interpretation, Vol. I: Analytical and Numerical Studies", Final Report to USAFSAM, Brooks AFB, Texas 78235 for contract F33615-78-C-0615, Scientific Systems, Inc., Cambridge, MA., Report S2I Tr 79-2, April, 1979.

(Gustafson, 1981)
D. E. Gustafson, J.-Y. Wang, and A. S. Willsky, "Cardiac Rhythm Interpretation Using Statistical P and R Wave Analysis", Frontiers of Engineering in Health Care, Houston, Sept., 1981.

(Haywood, 1970)
L. J. Haywood, V. K. Murthy, G. A. Harvey, and S. Saltzberg, "On-line Real Time Computer Algorithm for Monitoring the ECG Waveform", Comput. and Biomed. Res., Vol. 3, pp. 15-25, 1970.

(Hristov, 1971)
H. R. Hristov, G. B. Astardjian, and C. H. Nachev, "An Algorithm for the Recognition of Heart Rate Disturbances", Med. and Biol. Eng. (G. B.), Vol. 9, No. 3, pp. 221-227, May 1971.

(Katz, 1977)
A. M. Katz, Physiology of the Heart (New York: Raven Press, 1977).

(LeBlanc, 1973)
A. R. LeBlanc and F. A. Roberge, "Present State of Arrhythmia Analysis by Computer", Canadian Medical Assoc. J., Vol. 108, pp. 1239-1251, May, 1973.

(Marcus, 1982)
J. N. Marcus, "A Matched Filter Detector of QRS Complexes in Electrocardiograms", SB Thesis, Dept. of Electrical Engineering and Computer Science, M.I.T., Cambridge, MA., May, 1982.

(Marriott, 1977)
H. J. L. Marriott, Practical Electrocardiology (6th edition; Baltimore: Williams and Wilkins, 1977).

(McFee, 1972)
R. McFee and G. M. Baule, "Research in Electrocardiology and Magnetocardiology", Proc. IEEE, Vol. 60, No. 3, pp. 290-321, March, 1972.

(Miller, 1978a)
W. T. Miller and D. B. Geselowitz, "Simulation Studies of Electrocardiogram, Part 1: Normal Heart", Circul. Res., Vol. 43, No. 2, pp. 301-315, Aug., 1978.

(Miller, 1978b)
W. T. Miller and D. B. Geselowitz, "Simulation Studies of Electrocardiogram, Part 2: Ischemia and Infarction", Circul. Res., Vol. 43, No. 2, pp. 315-323, Aug., 1978.

(Moe, 1966)
G. K. Moe and C. Mendez, "Simulation of Impulse Propagation in Cardiac Tissue", Ann. NY Acad., Vol. 128, pp. 766-771, 1966.

(Murthy, 1979)
I. S. N. Murthy, M. R. Rangaraj, K. J. Udupa, and A. K. Goyal, "Homomorphic Analysis and Modeling of ECG Signals", IEEE Trans. on Biomed. Eng., Vol. BME-26, No. 6, pp. 330-344, June, 1979.

(Oliver, 1977)
G. C. Oliver, K. L. Ripley, J. P. Miller, and T. F. Martin, "A Critical Review of Computer Arrhythmia Detection" in Computer Electrocardiography: Present Status and Criteria, L. Prody (ed.) (Mount Kisco, NY: Futura Press, 1977), pp. 319-360.

(Plonsey, 1966)
R. Plonsey, "Limitations on the Equivalent Cardiac Generator", Biophys. J., Vol. 6, pp. 163-173, 1966.

(Plonsey, 1969)
R. Plonsey, Bioelectric Phenomena (New York: McGraw-Hill Book Co., 1969).

(Plonsey, 1971)
R. Plonsey, "The Biophysical Basis for Electrocardiography", CRC Critical Reviews in Bioengineering, Vol. 1, No. 1, pp. 1-48, Oct., 1971.

(Plonsey, 1979)
R. Plonsey, "Fundamentals of Electrical Processes in the Electrophysiology of the Heart" in Advances in Cardiovascular Physics Vol. 1: Theoretical Foundations of Cardiovascular Processes, D. N. Ghista, E. Van Vollenhoven, W.-J. Yang, and H. Revl (eds.) (Basel: S. Karger AG, 1979), pp. 1-28.

(Proceedings of the IEEE Computers in Cardiology Conference, 1974-1984)
Proc. of the 1974 Computers in Cardiology Conference, K. M. Kempner (ed.), Oct. 2-4, 1974, National Institutes of Health, Bethesda, Maryland, USA (new York: IEEE, 1974).
Proc. of the 1975 Computers in Cardiology Conference, K. M. Kempner (ed.), Oct. 2-4, 1975, Thoraxcentrum, Rotterdam, The Netherlands (New York: IEEE, 1975).
Proc. of the 1976 Computers in Cardiology Conference, H. G. Ostrow and K. L. Ripley (eds.), Oct. 7-9, 1976, Washington University, St. Louis, Missouri, USA (New York: IEEE, 1976).
Proc. of the 1977 Computers in Cardiology Conference, H. G. Ostrow and K. L. Ripley (eds.), Sept. 29-Oct. 1, Thoraxcentrum, Rotterdam, The Netherlands (New York: IEEE, 1977).
Proc. of the 1978 Cimputers in Cardiology Conference, K. L. Ripley and H. G. Ostrow (eds.), Sept. 12-14, 1978, Stanford University, Stanford, California, USA (New York: IEEE, 1978).
Proc. of the 1979 Computers in Cardiology Conference, K. L. Ripley and H.G. Ostrow (eds.), Sept. 26-28, 1979, Cardiology Center, University of Geneva, Geneva, Switzerland (new York: IEEE, 1979).
Proc. of the 1980 Computers in Cardiology Conference, K.L. Ripley and H. G. Ostrow (eds.), Oct. 22-24, 1980, Williamsburg, Virginia, USA (New York: IEEE, 1980).
Proc. of the 1981 Computers in Cardiology Conference, K. L. Ripley (ed.), Sept. 23-25, 1981, Florence, Italy (New York: IEEE, 1982).
Proc. of the 1982 Computers in Cardiology Conference, K. L. Ripley (ed.), Oct. 12-15, 1982, Seattle, Washington, USA (New York: IEEE, 1983).
Proc. of the 1983 Computers in Cardiology Conference, K. L. Ripley (ed.), Oct. 4-7, 1983, Aachen, Germany (New York: IEEE, 1983).
Proc. of the 1984 Computers in Cardiology Conference, K. L. Ripley (ed.), Sept. 18-21, Salt Lake City, Utah, USA (New York: IEEE, 1984).

(Richardson, 1971)
J. M. Richardson, L. J. Haywood, V. K. Murthy, and R. E. Kalaba, "A Decision Theoretic Approach to the Detection of ECG Abnormalities, Part II: Approximate Treatment of the Detection of Ventricular Extrasystoles", Math. Biosci. (USA), Vol. 12 Nos. 1-2, pp. 97-103, Oct. 1971.

(Rosenberg, 1972)
R. M. Rosenberg. C. H. Chao, and J. Abbott, A New Mathematical Model of Electrical Cardiac Activity", Math. Biosci. (USA), Vol. 14, Nos. 3-4, pp. 367-394, Aug., 1972.

(Shah, 1977)
P. M. Shah, J. M. Arnold, N. A. Haberern, D. T. Bliss, K. M. McClelland, and W. B. Clarke, "Automatic Real Time Arrhythmia Monitoring in the Intensive Coronary-Care Unit", Am. J. Card., Vol. 39, No. 5, pp. 701-708 May 4, 1977.

(Smith, 1982)
J. M Smith, "Finite Element Model of Ventricular Dysrhythmias", MS Thesis, Dept. of Electrical Engineering and Computer Science, M.I.T., Cambridge, MA., Aug., 1982.

(Sornmo, 1981)
L. Sornmo, P. O. Borjesson, M.-E. Nygards, and O. Pahlm, "A Method for Evaluation of QRS Shape Features Using a Mathematical Model for the ECG", IEEE Trans. on Biomed. Eng., Vol. BME-28, No. 10, pp. 713-717, Oct., 1981.

(Thiry, 1974)
P. S. Thiry and R. M. Rosenberg, "On Electrophysiological Activity of the Normal Heart", J. of the Franklin Institute, Vol. 297, No. 5, pp. 377-396, May, 1974.

(Thiry, 1975)
P. S. Thiry, R. M. Rosenberg, and J. A. Abbott, "A Mechanism for the Electrocardiogram Response to Left Ventricular Hypertrophy and Acute Ischemia", Circul. Res., Vol. 36, No. 1, pp. 92-104, Jan., 1975.

(Thomas, 1979)
L. J. Thomas Jr., K. W. Clark, C. N. Mead, K. L. Ripley, B. F. Spenner, and G. C. Oliver Jr., "Automated Cardiac Dysrhythmia Analysis", Proc. IEEE, Vol. 57, No. 9, pp. 1322-1337, Sept., 1979.

(Tripp, 1979)
J. H. Tripp, "Theory of the Magnetocardiogram" in Advances in Cardiovascular Physics, Vol. 1: Theoretical Foundations of Cardiovascular Processes, D. N. Ghista, E. Vanvollenhoven, W. J. Yang, and H. Real (eds.) (Basel: S. Karger AG, 1979), pp. 29-46.

(Tsui, 1975)
E. T. Tsui and E. Wong, "Sequential Approach to Heart-Beat Rhythm Classification", IEEE Trans. on Info. Theory, Vol. IT-21, No. 5, pp. 596-599, Sept., 1975.

(Uijen, 1979)
G. J. H. Uijen, J. P. C. de Weerd, and A. J. H. Vendrik, "Accuracy of QRS Detection in Relation to the Analysis of High Frequency Components in the Electrocardiogram", Med. and Biol. Eng. and Comput. (G. B.), Vol. 17, No. 4, pp. 492-502, July, 1979.

(Vinke, 1977)
R. V. H. Vinke, A. C. Arntzenius, P. H. Huisman, H. E. Kulbertus, H. J. Ritsema van Eck, J. J. Schipperheijn, and M. L. Simoons, "Evaluation of a Computer Model of Ventricular Excitation", Proc. Computers in Cardiology 1977, pp. 605-610, 1977.

(White, 1976)
C. C. White, "Note on a Markov Chain Approach to Cardiac-Arrhythmia Classification", Comput. Biomed. Res., Vol. 9, No. 6, pp. 503-506, 1976.

(Wikswo, 1979)
J. P. Wikswo Jr., J. A. V. Malmivuo, W. H. Barry, M. C. Leifer, and W. M. Fairbank, "The Theory and Application of Magnetocardiography" in Advances in Cardiovascular Physics, Vol. 2: Cardiograms: Theory and Application, D. N. Ghista, E. Van Vollenhoven, W.-J. Yang, and H. Reul (eds.) (Basel: S. Karger AG, 1979), pp. 1-67.

(Zloof, 1973)
M. Zloof, R. M. Rosenberg, and J. Abbott, "A Computer Model for Atrioventricular Blocks", Math. Biosci. (USA), Vol. 18, pp. 87-117, 1973.

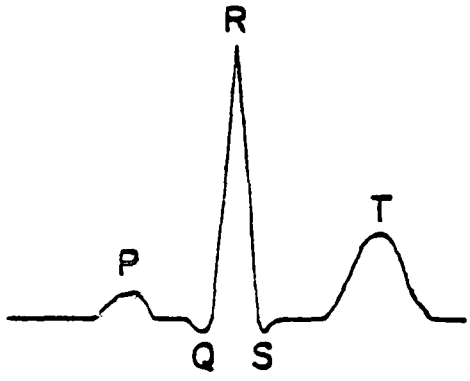

Figure 1. Wave form Definitions for One Beat of an Idealized, Normal ECG.

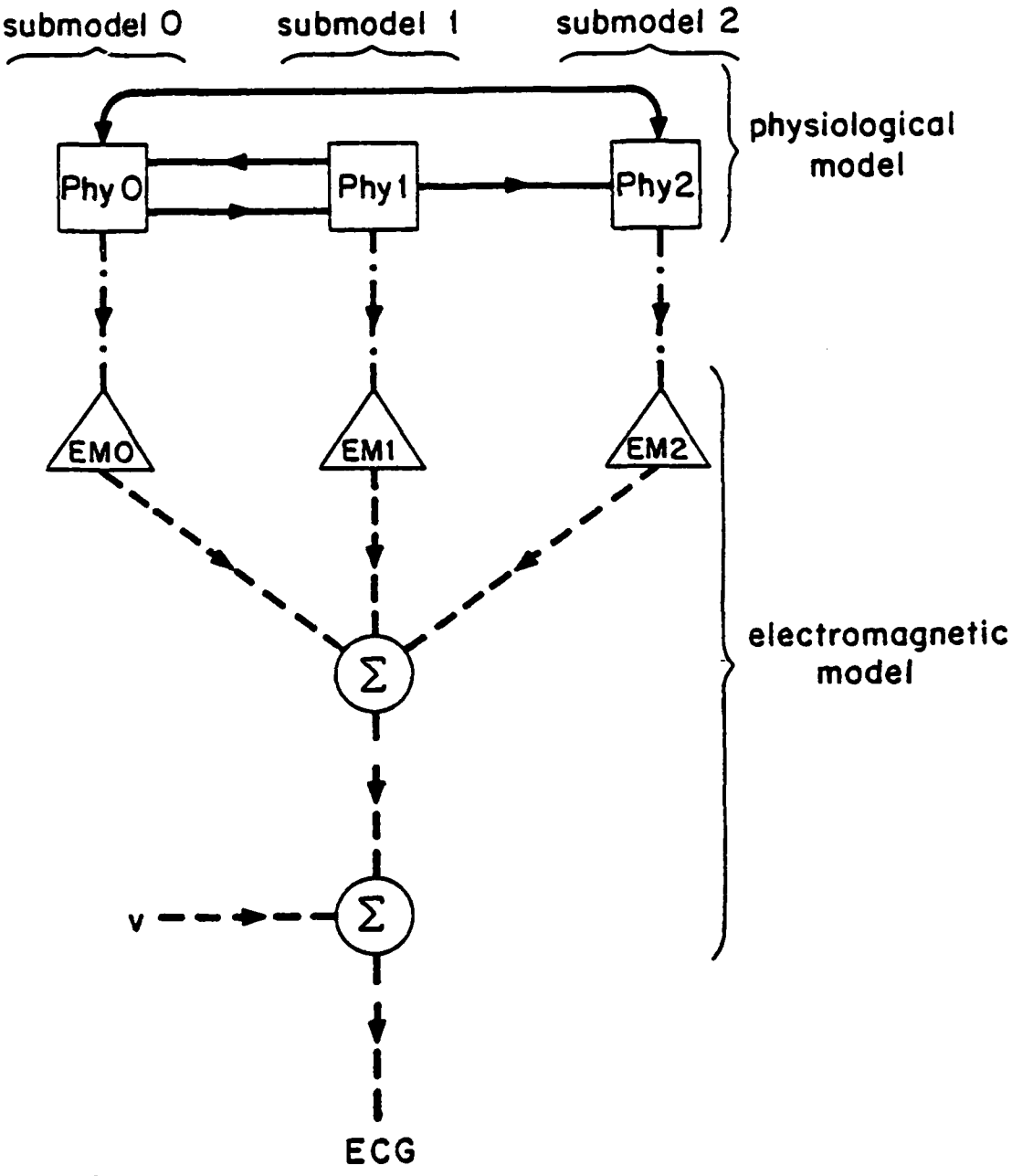

Figure 2. Spatial and Hierarchical Decompositions.

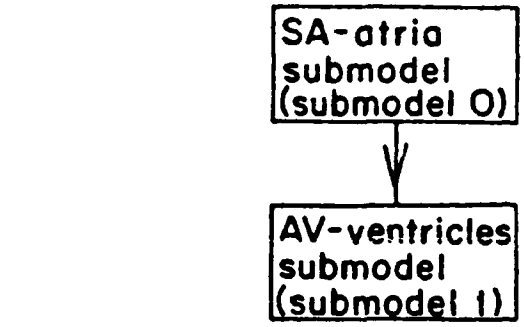

(a)

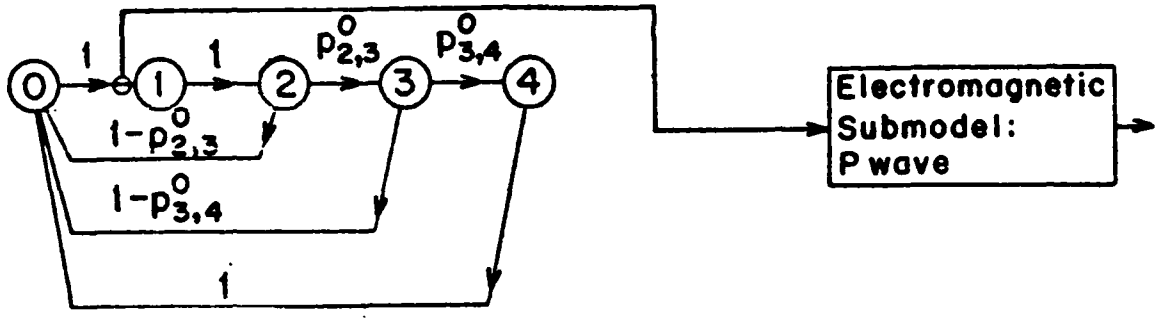

(b)

If the state of the SA-atrial submodel $\in \{0, 2, 3, 4\}$: (c)

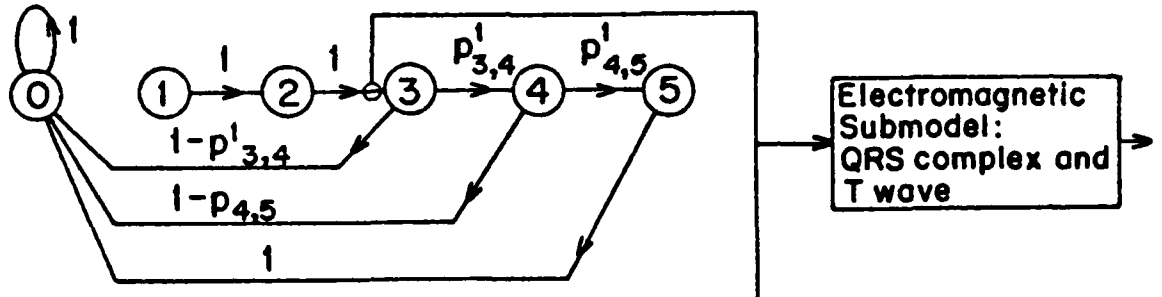

If the state of the SA-atrial submodel $\in \{1\}$:

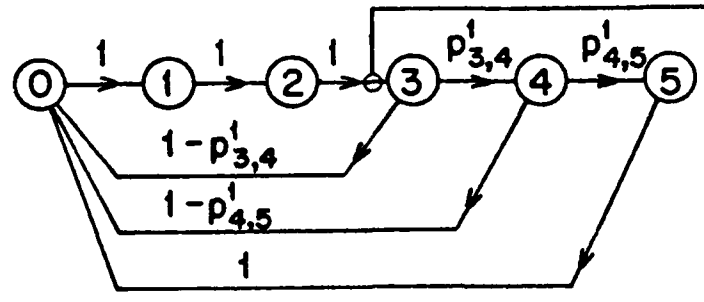

Figure 3. A Simple Model for Normal Rhythm.
(a) Submodel Block Diagram.
(b) SA-atrial Submodel.
(c) AV-ventricular Submodel.

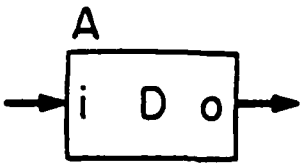

Figure 4. Delay Line Symbol.
i = initial state and o = final state.

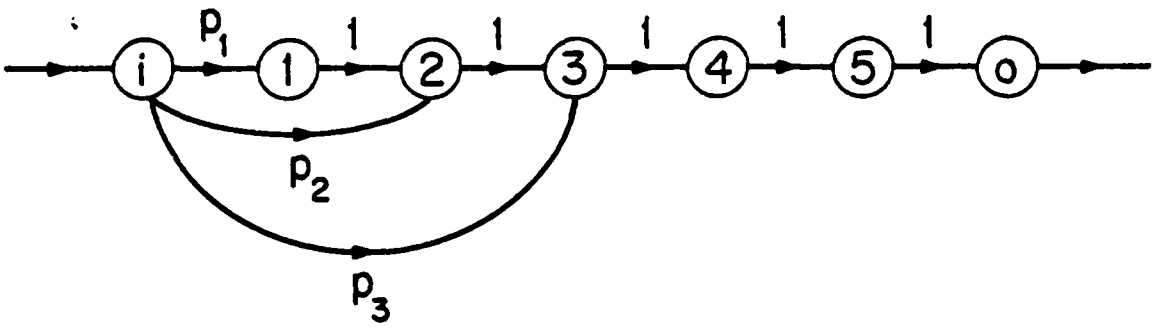

(a)

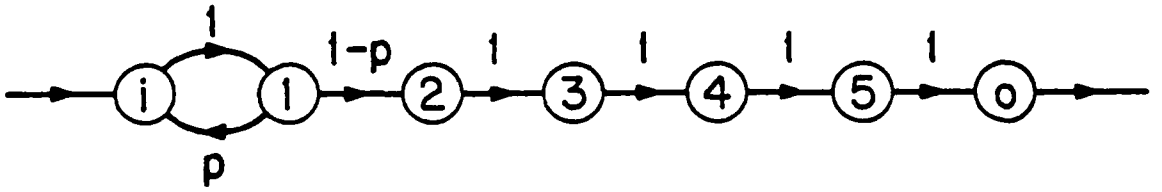

(b)

Figure 5 Examples of Delay Lines.
(a) Without Feedback Transition.
(b) With Feedback Transitions.

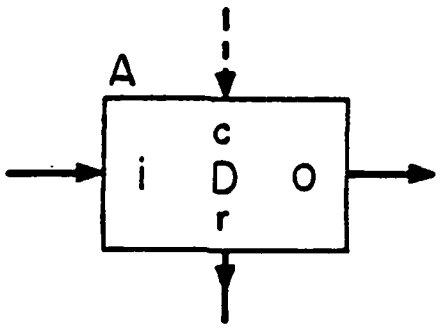

Figure 6. Resettable Delay Line Symbol.
i = input, o = normal output, r = reset output, and c = control input.

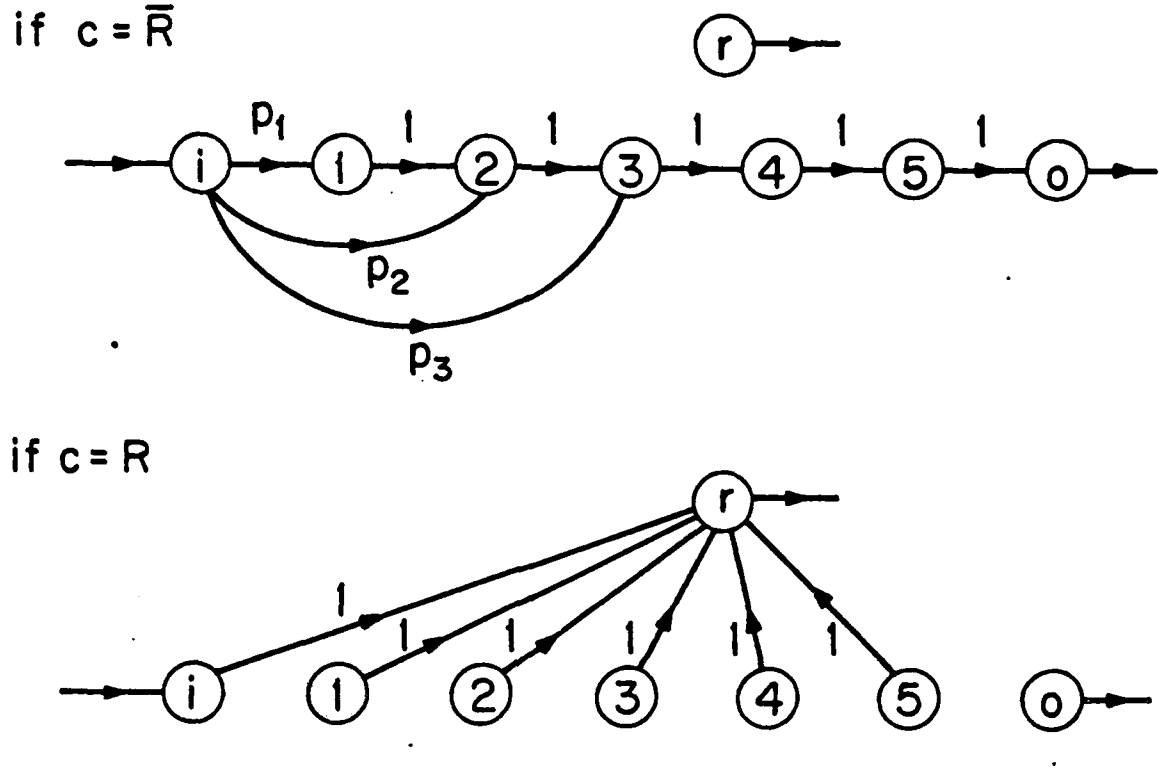

Figure 7. An example of Resetable Delay Line and its Reset State r.

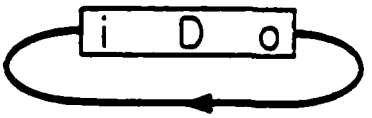

Figure 8. Basic Autorhythmic Element.

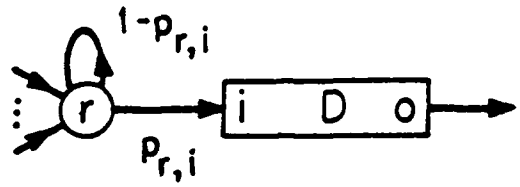

Figure 9. Passive Transmission Line.

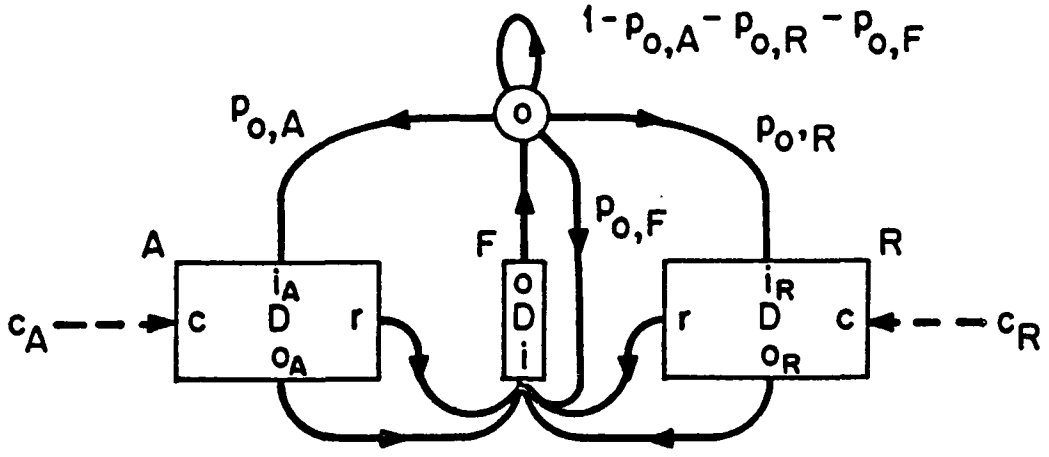

Figure 10. Bidirectional Refractory Transmission Line.

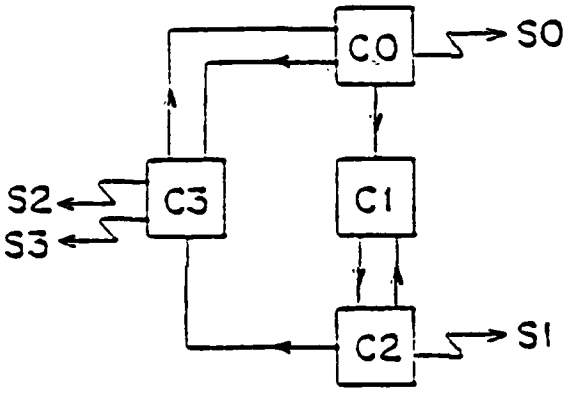

Figure 11. An Illustration of the Block Diagram Description of a Class of Models.

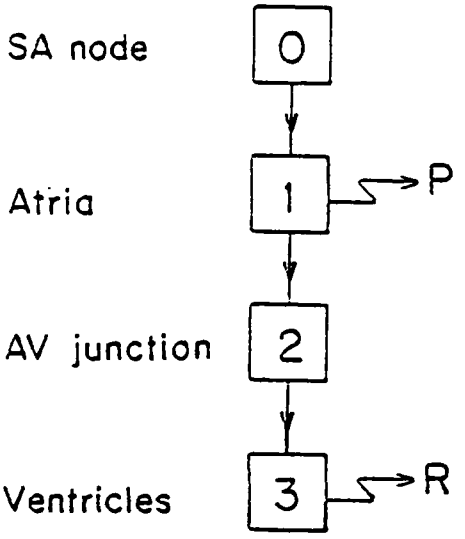

Figure 12. A Model for Normal Rhythm.
Part (a): Submodel Structure.

Submodel 0: SA-nodal Substructure

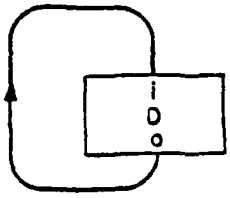

Submodel 1: Atrial Substructure

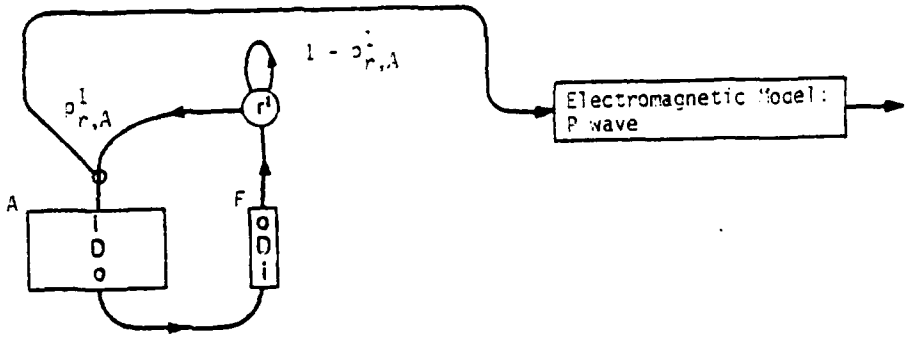

Submodel 2: AV-junctional Substructure

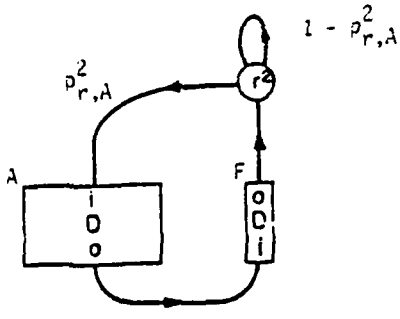

Submodel 3: Ventricular Substructure

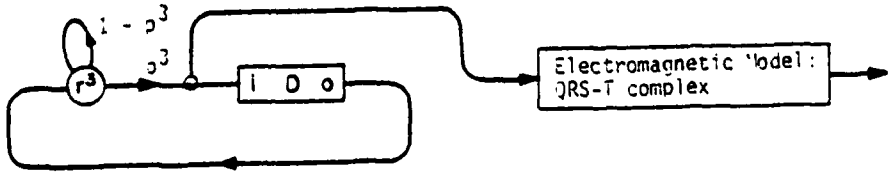

Figure 12. Continued.
Part (b): Block Diagram.

Submodel 0:

Submodel for the SA-nodal Substructure

This submodel is autonomous.

Submodel 1:

Submodel for the Atrial Substructure

$$p^1_{r,A} = \begin{cases} 1 \text{ if } x^0 \in \{o^0\} \\ 0 \text{ otherwise} \end{cases}$$

Submodel 2:

Submodel for the AV-junctional Substructure

$$p^2_{r,A} = \begin{cases} 1 \text{ if } x^1 \in \{o^1_A\} \\ 0 \text{ otherwise} \end{cases}$$

Submodel 3:

Submodel for the Ventricular Substructure

$$p^3 = \begin{cases} 1 \text{ if } x^2 \in \{o^2_A\} \\ 0 \text{ otherwise} \end{cases}$$

Figure 12 Continued.
Part (c): Intersubmodel Interactions.

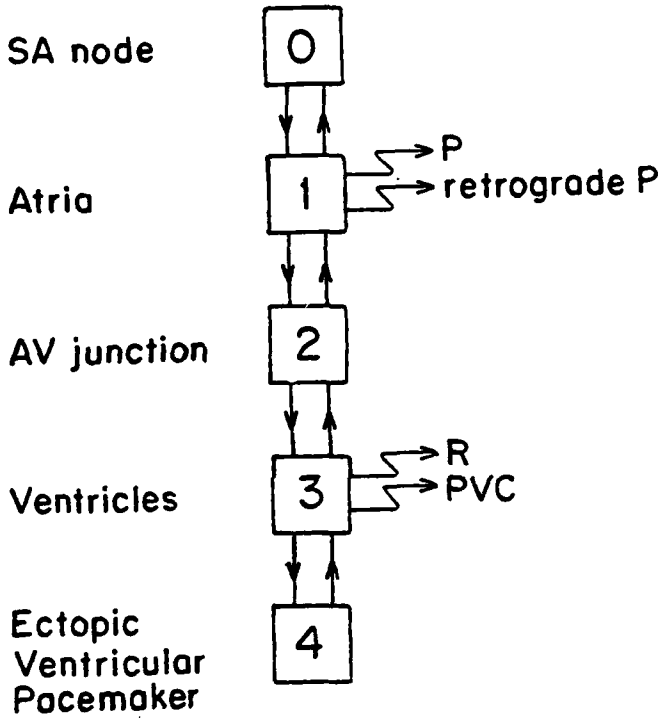

Figure 13. A Model for Normal Rhythm with PVCs Generated by an Ectopic Focus.
Part (a): Submodel Structure.

Submodel 0: SA-nodal Substructure

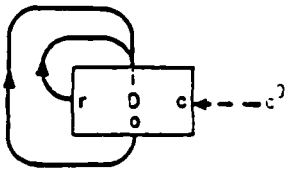

Submodel 1: Atrial Substructure

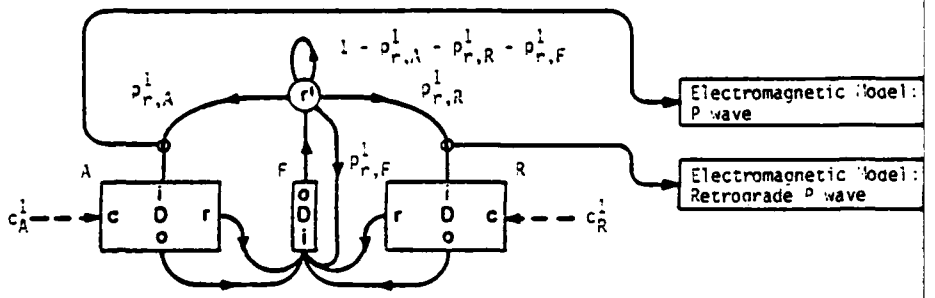

Submodel 2: AV-junctional Substructure

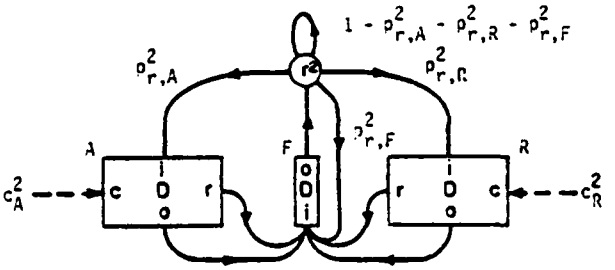

Submodel 3: Ventricular Substructure

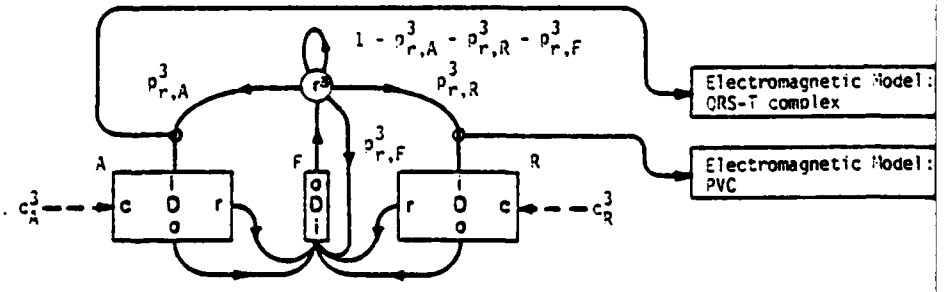

Submodel 4: Ectopic-ventricular-pacemaker Substructure

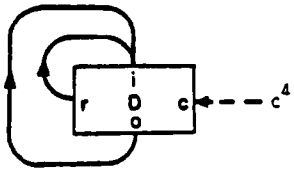

Figure 13. Continued.
Part (b): Block Diagram.

Submodel 1:

Submodel for the Atrial Substructure

$$p^1_{r,A} = \begin{cases} 1 \text{ if } x^0 \in \{o^0\} \text{ and } x^2 \in \{o^2_R\} \\ 0 \text{ otherwise} \end{cases}$$

$$p^1_{r,R} = \begin{cases} 1 \text{ if } x^0 \in \{o^0\} \text{ and } x^2 \in \{o^2_R\} \\ 0 \text{ otherwise} \end{cases}$$

$$p^1_{r,F} = \begin{cases} 1 \text{ if } x^0 \in \{o^0\} \text{ and } x^2 \in \{o^2_R\} \\ 0 \text{ otherwise} \end{cases}$$

$$c^1_A = \begin{cases} \bar{R} \text{ if } x^2 \in \{o^2_R\} \\ R \text{ otherwise} \end{cases}$$

Figure 13. Continued.
Part (c): Intersubmodel Interactions. These interactions are similar to those of the Normal Rhythm model described in Figure 12. Therefore, only the interactions for submodel 1 are given.

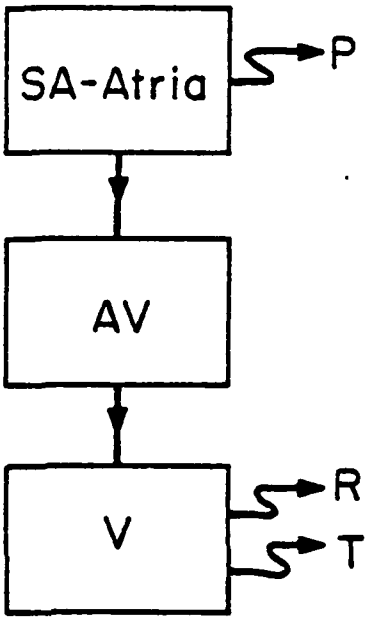

Figure 14. A Model For Wenckebach. Submodel Structure.

SA-Atria : x^0

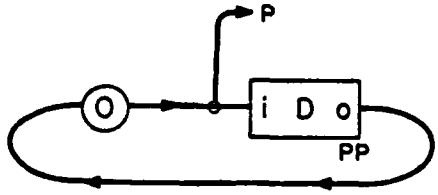

AV: x^1

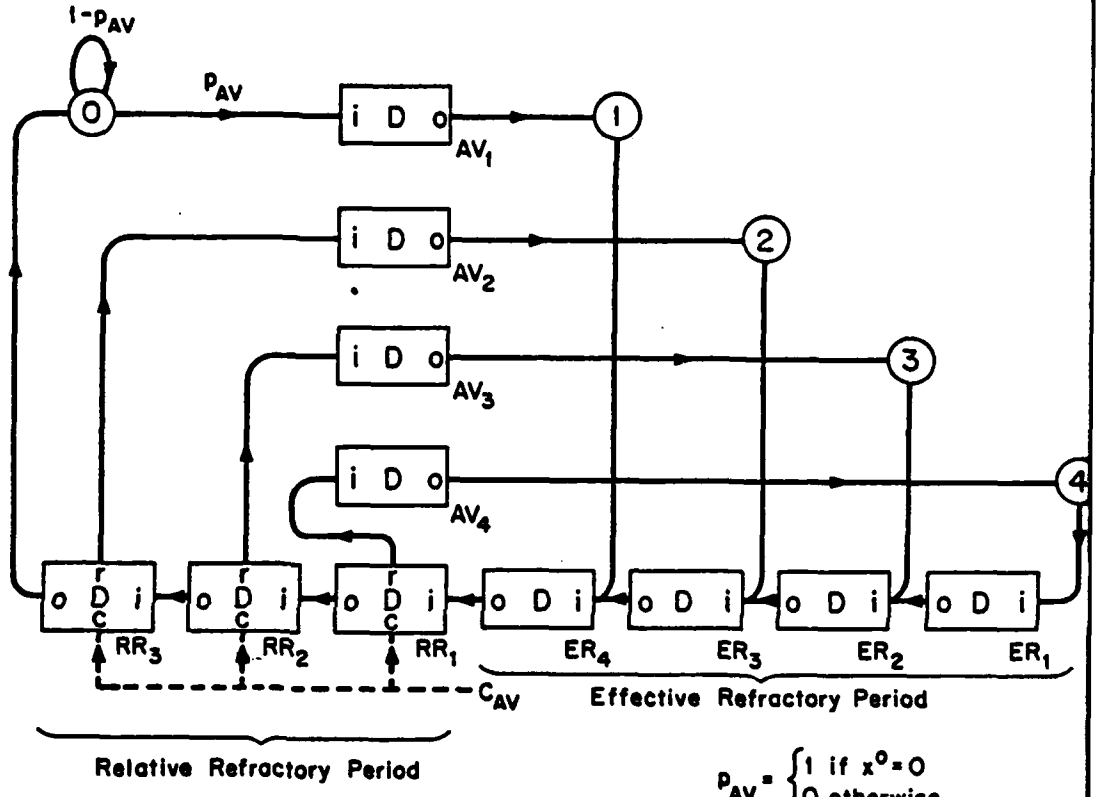

$$p_{AV} = \begin{cases} 1 \text{ if } x^0 = 0 \\ 0 \text{ otherwise} \end{cases}$$

$$C_{AV} = \begin{cases} R \text{ if } x^0 = 0 \\ \bar{R} \text{ otherwise} \end{cases}$$

Ventricles : x^2

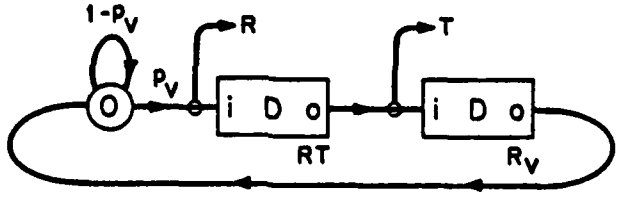

$$p_V = \begin{cases} 1 \text{ if } x^1 \in \{1,2,3,4\} \\ 0 \text{ otherwise} \end{cases}$$

Figure 15. A Model for Wenckebach. Block Diagram.

SA - Atrial : x^0

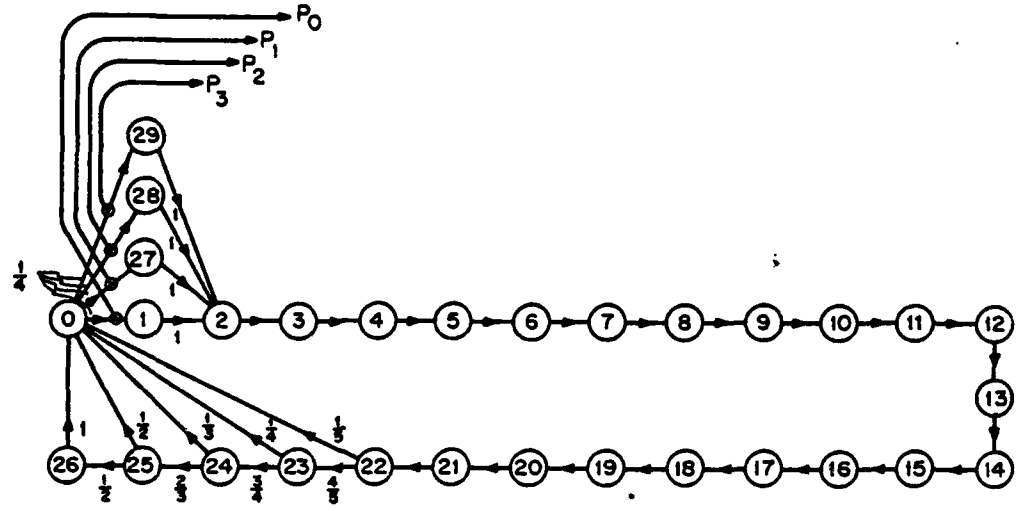

AV: x^1

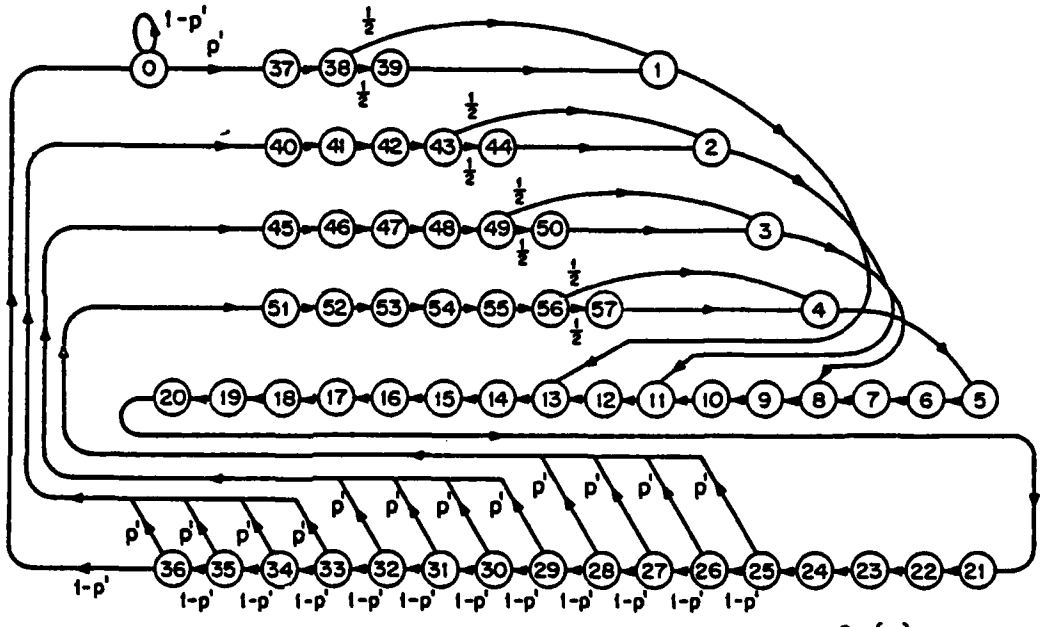

Ventricular: x^2

$$p' \begin{cases} 1 \text{ if } x^0 \in \{0\} \\ 0 \text{ otherwise} \end{cases}$$

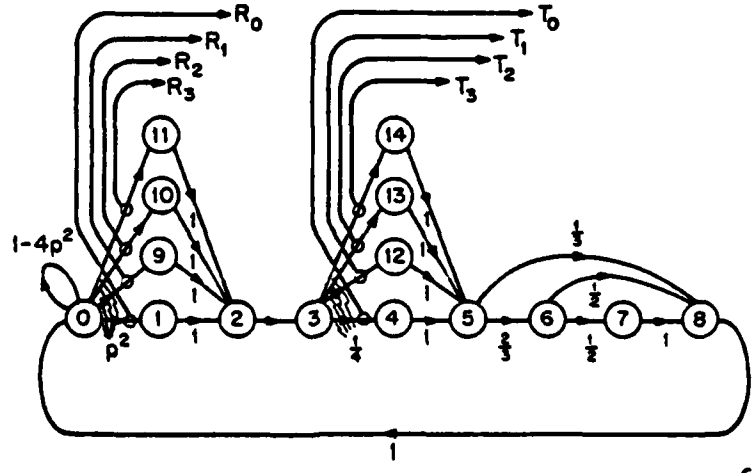

$$p^2 = \begin{cases} .25 \text{ if } x^1 \in \{1,2,3,4\} \\ 0 \text{ otherwise} \end{cases}$$

Figure 16. A Model For Wenckebach.
Markov Chains.

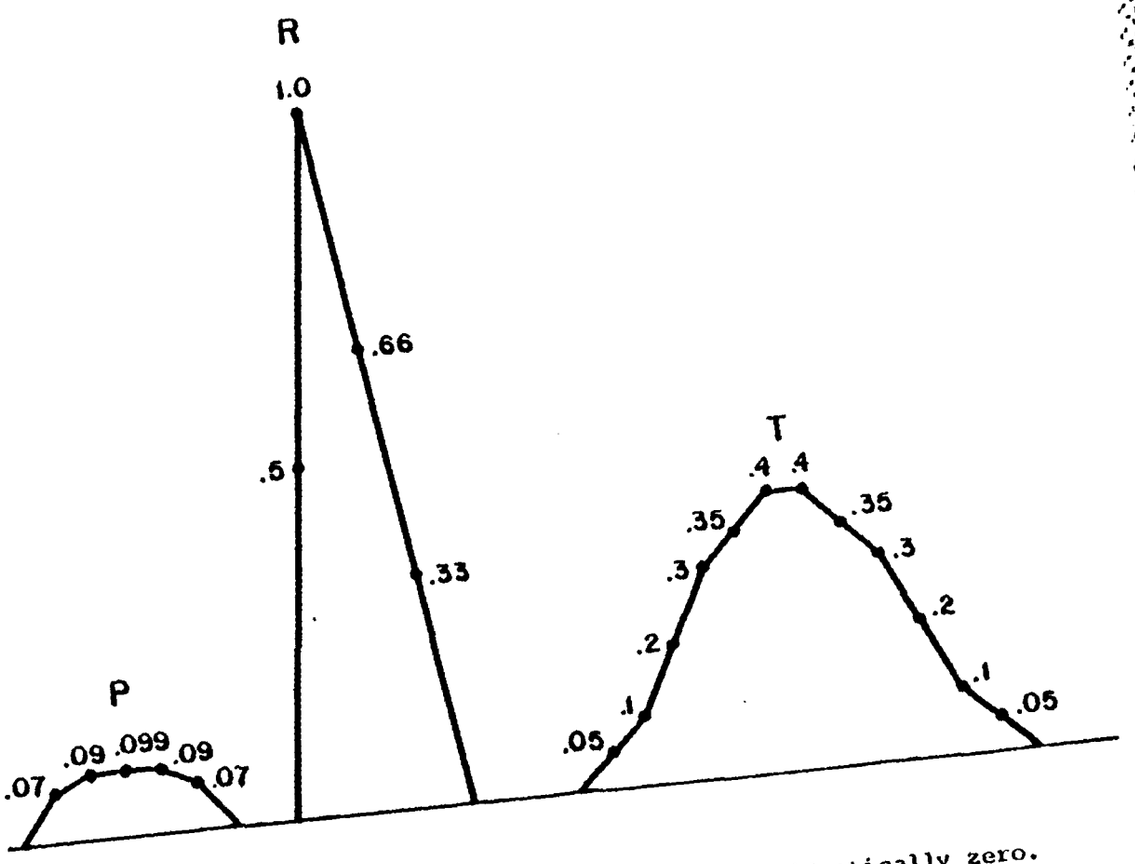

The covariances for the P, R, and T waves are all identically zero.

The X_i waves where $X \in P,R,T$ and $i \in 0,1,2,3$ are defined to be

$$X_i(n) = X(n-i).$$

Figure 16. Continued.
Signatures.

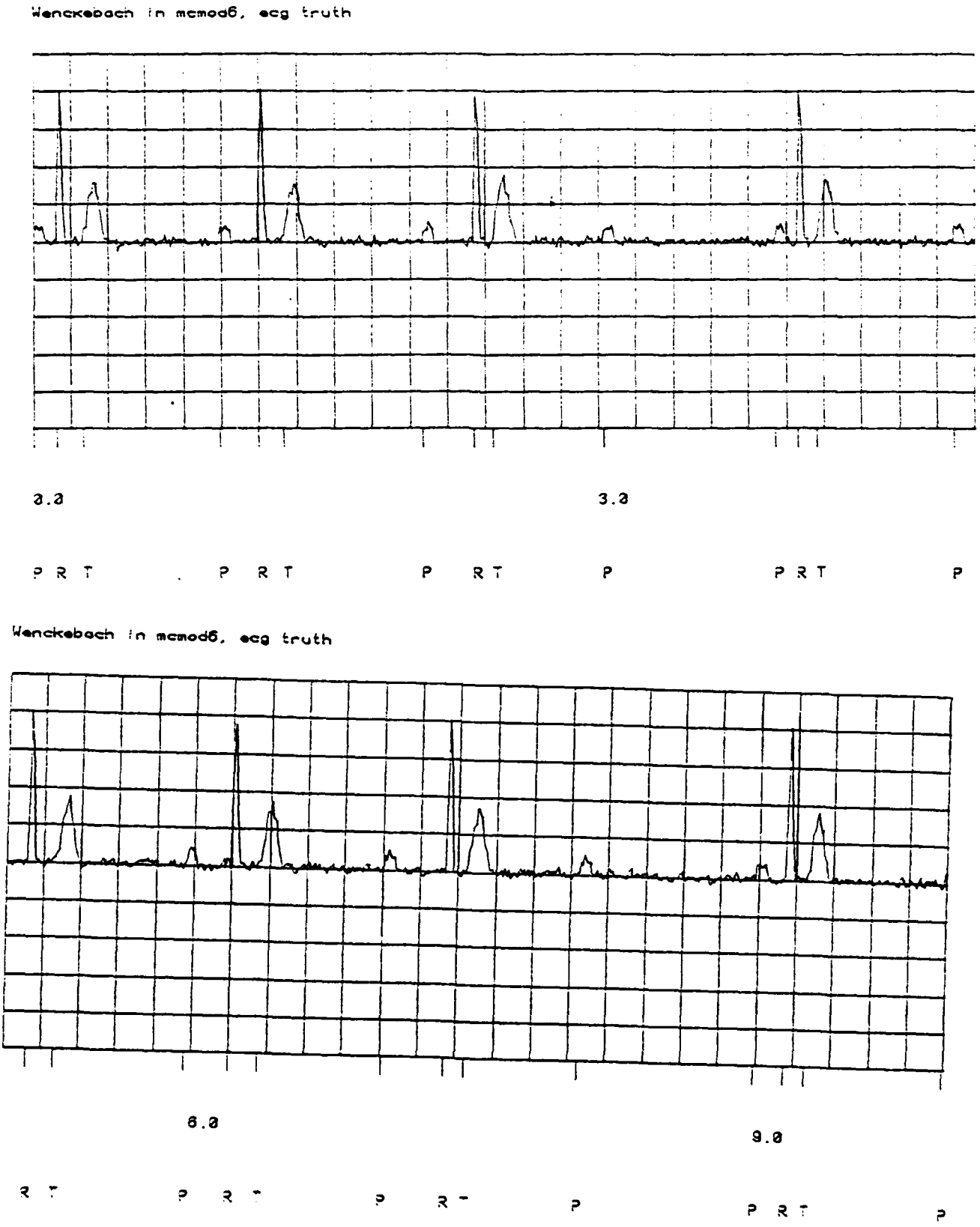

Figure 17. Wenckebach: ECG.
The interval data for this simulated ECG is tabultaed in Table 1.

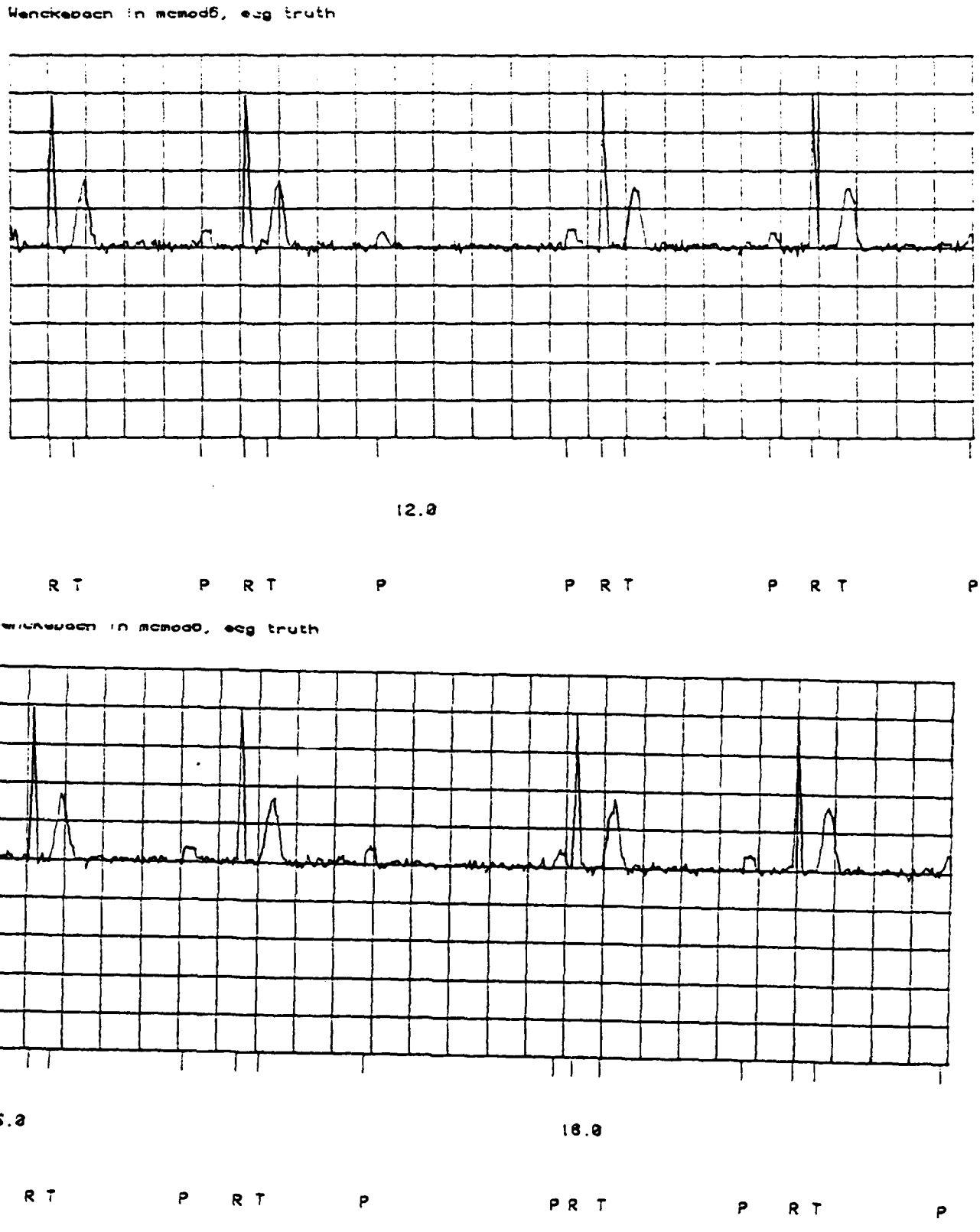

Figure 17. Continued.

P wave Number	Time (sec.)	P-R Interval (sec.)	Time Since Last P wave (sec.)
0	0	.13	
1	.99	.21	.99
2	2.07	.27	1.08
3	3.03	dropped	.96
4	3.94	.12	.91
5	4.89	.23	.95
6	5.96	.24	1.07
7	7.01	.33	1.05
8	8.05	dropped	1.04
9	8.99	.16	.94
10	9.99	.22	1
11	10.99	.23	1
12	11.91	dropped	.92
13	12.89	.18	.98
14	13.94	.22	1.05
15	14.98	.24	1.04
16	16.02	.28	1.04
17	16.96	dropped	.94
18	17.95	.09	.99
19	18.93	.26	.98
20	19.96	.3	1.03

Table 1. Wenckebach: P-P and P-R Intervals.
The simulated ECG from which this interval data was computed is shown in Figure 17.

END

FILMED

1-86

DTIC